Biomacromolecules

Article

pubs.acs.org/Biomac

Assessment of Cholesterol-Derived *Ionic* Copolymers as Potential Vectors for Gene Delivery

Sema Sevimli,[†,‡] Sharon Sagnella,[†,§] Maria Kavallaris,[†,§] Volga Bulmus,*[,∥] and Thomas P. Davis*[,⊥,#]

[†]Australian Centre for Nanomedicine (ACN), The University of New South Wales, Sydney, New South Wales 2052, Australia

[‡]The Centre for Advanced Macromolecular Design (CAMD), The University of New South Wales, Sydney, New South Wales 2052, Australia

[§]Children's Cancer Institute Australia (CCIA), Lowy Cancer Research Centre, The University of New South Wales, Sydney, New South Wales 2052, Australia

[∥]Department of Chemical Engineering, Biotechnology and Bioengineering Graduate Program, Izmir Institute of Technology, Urla, Izmir 35430, Turkey

[⊥]Monash Institute of Pharmaceutical Sciences, Monash University, Parkville, Melbourne, Victoria 3052, Australia

[#]Department of Chemistry, University of Warwick, Coventry West Midlands CV4 7AL, U.K.

Supporting Information

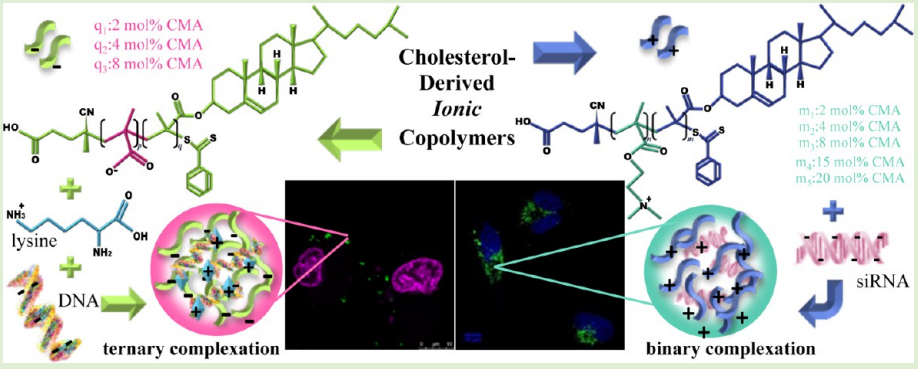

ABSTRACT: A library of cholesterol-derived *ionic* copolymers were previously synthesized via reversible addition−fragmentation chain transfer (RAFT) polymerization as 'smart' gene delivery vehicles that hold diverse surface charges. Polyplex systems formed with anionic poly(methacrylic acid-co-cholesteryl methacrylate) (P(MAA-*co*-CMA)) and cationic poly(dimethylamino ethyl methacrylate-co-cholesteryl methacrylate) (Q-P(DMAEMA-*co*-CMA)) copolymer series were evaluated for their therapeutic efficiency. Cell viability assays, conducted on SHEP, HepG2, H460, and MRC5 cell lines, revealed that alterations in the copolymer composition (CMA mol %) affected the cytotoxicity profile. Increasing the number of cholesterol moieties in Q-P(DMAEMA-*co*-CMA) copolymers reduced the overall toxicity (in H460 and HepG2 cells) while P(MAA-*co*-CMA) series displayed no significant toxicity regardless of the CMA content. Agarose gel electrophoresis was employed to investigate the formation of stable polyplexes and determine their complete conjugation ratios. P(MAA-*co*-CMA) copolymer series were conjugated to DNA through a cationic linker, oligolysine, while Q-P(DMAEMA-*co*-CMA)-siRNA complexes were readily formed via electrostatic interactions at conjugation ratios beginning from 6:1:1 (oligolysine-P(MAA-*co*-CMA)-DNA) and 20:1 (Q-P(DMAEMA-*co*-CMA)-siRNA), respectively. The hydrodynamic diameter, ζ potential and complex stability of the polyplexes were evaluated in accordance to complexation ratios and copolymer composition by dynamic light scattering (DLS). The therapeutic efficiency of the conjugates was assessed in SHEP cells via transfection and imaging assays using RT-qPCR, Western blotting, flow cytometry, and confocal microscopy. DNA transfection studies revealed P(MAA-*co*-CMA)-oligolysine-DNA ternary complexes to be ineffective transfection vehicles that mostly adhere to the cell surface as opposed to internalizing and partaking in endosomal disrupting activity. The transfection efficiency of Q-P(DMAEMA-*co*-CMA)-GFP siRNA complexes were found to be polymer composition and N/P ratio dependent, with Q-2% CMA-GFP siRNA polyplexes at N/P ratio 20:1 showing the highest gene suppression in GFP expressing SHEP cells. Cellular internalization studies suggested that Q-P(DMAEMA-*co*-CMA)-siRNA conjugates efficiently escaped the endolysosomal pathway and released siRNA into the cytoplasm. The gene delivery profile, reported herein, illuminates the positive and negative attributes of each therapeutic design and strongly suggests Q-P(DMAEMA-*co*-CMA)-siRNA particles are extremely promising candidates for *in vivo* applications of siRNA therapy.

Received: September 1, 2013
Revised: October 11, 2013
Published: October 14, 2013

INTRODUCTION

Gene therapy, a promising approach for the treatment of viral infections, cancers, cardiovascular and neurodegenerative diseases[1,2] is governed by the efficiency and safety of the gene carrier.[3] Nonviral gene delivery systems, for instance, polymers, offer several advantages over viral vectors, such as less immunogenicity, larger gene-loading capacity and lower cost,[4−7] making them ideal candidates for gene therapy.

Most therapeutic strategies rely on the distribution of their therapeutic materials reaching the intracellular sites at effective concentrations while protecting the therapeutic from nuclease degradation.[8,9] One of the main obstacles that these systems encounter is the cellular membrane transport barrier.[10] Therapeutic systems are expected to efficiently destabilize the cell membrane and facilitate the delivery of their cargo to the cytosol and/or nucleus. Upon external stimulation, such as acidification in the endosomal environment, 'smart' pH-responsive polymers are able to change their conformation from an expanded hydrophilic coil (at physiological pH) to a relatively less hydrophilic globule (at acidic pH) and destabilize/disrupt the phospholipid cell membrane.[11] Owing to their membrane disrupting properties, pH-responsive polymers have been widely investigated as therapeutic delivery systems.[12−15] A number of carboxylated amphiphatic polymers such as poly(ethyl acrylic acid) (PEAA),[16] poly(propyl acrylic acid) (PPAA),[9,13] poly(butyl acrylic acid) (PBAA),[14] poly(acrylic acid/ethyl acrylate) (P(AA/EA)),[9] poly(acrylic acid/propyl acrylate) (P(AA/PA)),[13] poly(methacrylic acid/butyl acrylate) (P(MAA/BA)),[8] poly(methacrylic acid/*N*-isopropyl acrylamide/octadecyl acrylate) (P(MAA/NIPAA/ODA)),[17] and poly(methacrylic acid/butyl acrylate/pyridyldisulfide acrylate) (P(MAA/BA/PDSA))[8] have been described to reorganize the lipid bilayer of membranes in a pH-dependent manner. Endosomal membrane-disrupting polyanions have been investigated as gene delivery agents in the form of ternary polyplexes, where the anionic components are brought together by a cationic molecule, achieving promising results.[18−20]

A different approach to escape the endosomal barrier and enable cytosolic delivery of genes is through the use of cationic polymers. Certain cationic polymers stimulate membrane destabilization by a mechanism called the 'proton-sponge effect',[21] where the high buffering capacity of polycations leads to increase in pH of the endosomes, accumulating ions within this compartment, and causing osmotic swelling that eventually bursts the vesicle.[22] Polycations spontaneously interact with negatively charged therapeutic entities, such as siRNA or DNA, and form polyelectrolyte complexes, also known as polyplexes.[23] However, for efficient gene complexation, polycations are required to carry high charge densities along with high molecular weights, which often causes carrier-induced toxicity and undesired aggregation.[24] Utilizing biodegradable/reducible polycations (such as poly(*β*-amino ester)s, poly(spermine)s, poly(amido amine)s),[25] incorporating hydrophobic moieties,[26] altering the polymer properties with poly-(ethylene glycol) (PEG) conjugation[27] are some of the common strategies employed to lower the cytotoxicity and enhance the stability of polyplexes.[28−30]

The aim of this study is to biologically evaluate the intracellular gene delivery performance of CMA-derived ionic copolymer series—P(MAA-*co*-CMA) (as pH-responsive anionic polymer series) and Q-P(DMAEMA-*co*-CMA) (as stimuli responsive cationic polymer series)—in cancer cell lines and normal cells. Considering the ability of cholesterol to cross cellular membranes, cholesterol units were separately fused with PMAA, to switch the cell-membrane activity of cholesterol on or off in a pH-dependent manner, and PDMAEMA polymers, to reduce the overall toxicity caused by the tertiary amines, in order to provide site-selective membrane destabilization activity in endosomes/lysosomes and cytosolic-release of the therapeutic load. Gene transfection activity of polymer−gene complexes were investigated using *in vitro* cultured human neuroblastoma SHEP cells (cells that stably express green fluorescent protein (GFP) were utilized in siRNA delivery, while GFP expressing (pmaxFP-GreenC) plasmids were transfected in non-GFP SHEP cells). The influence of the macromolecular structure—especially variances in surface charge and polymer composition (CMA ratio)—on gene complexation ratios and the biochemical properties of the resulting polyplexes were examined in detail. The physicochemical properties of complexes; specifically their transfection efficiency, endosomolytic activity and intracellular delivery profiles were assessed in relation to the copolymer series.

EXPERIMENTAL SECTION

Materials. The procedure for the RAFT-mediated polymerizations of anionic P(MAA-*co*-CMA) (**A-2% CMA**, cholesterol content 2 mol %, with number average molecular weight $(M_n)_{GPC}$ of 16500 g/mol and polydispersity index (*PDI*) of 1.19; **A-4% CMA**, cholesterol content 4 mol %, with $(M_n)_{GPC}$ 15800 g/mol and *PDI* 1.10; **A-8% CMA**, cholesterol content 8 mol %, with $(M_n)_{GPC}$ 18000 g/mol and *PDI* 1.11) copolymer series has been previously described.[31] The preparation of quarternized-P(DMAEMA-*co*-CMA) copolymer series with varying CMA units (**Q-2% CMA**, cholesterol content 2 mol %, with $(M_n)_{GPC}$ 23400 g/mol and *PDI* 1.13; **Q-4% CMA**, cholesterol content 4 mol %, with $(M_n)_{GPC}$ 24800 g/mol and *PDI* 1.15; **Q-8% CMA**, cholesterol content 8 mol %, with $(M_n)_{GPC}$ 19200 g/mol and *PDI* 1.14; **Q-15% CMA**, cholesterol content 15 mol %, with $(M_n)_{GPC}$ 21400 g/mol and *PDI* 1.16; **Q-20% CMA**, cholesterol content 20 mol %, with $(M_n)_{GPC}$ 16000 g/mol and *PDI* 1.17) is presented in Supporting Information (Figure S1 and Table S1). Dulbecco's Modified Eagle Medium (DMEM) with 4.5 g/L glucose and L-glutamine, Roswell Park Memorial Institute (RPMI) medium with HEPES and L-glutamine, heat inactivated Fetal Calf Serum (FCS), trypsin solution (0.25% (w/v) trypsin in Hank's solution), Trypan Blue, Opti-MEM I Reduced Serum Medium, Lipofectamine 2000 and Geneticin were purchased from Invitrogen Life Technologies. *In vivo* custom antienhanced green fluorescence protein (anti-GFP) siRNA (sense strand; 5′-GCAAG-CUGACCCUGAAGUUCAU-3′; antisense, 5′-GAACUUCAG-GGUCAGCUUGCCG-3′) (14100 g/mol) was synthesized by Thermo Scientific Dharmacon. pmaxFP-GreenC was obtained from Lonza and TUBB-pREP4 plasmid (13.1 kb) was generated in the CCIA laboratories. AlexaFlour488 conjugated siRNA and *β*2 microglubin (*β*2M) primer mixes (forward + reverse) were obtained from Qiagen. High Capasity cDNA Reverse Transcription Kit (200 Reactions) and SYBR green kit were purchased from Applied Biosystems. Methyl iodide (Sigma), phosphate buffered saline (PBS; Sigma), oligolysine (1300 g/mol; Mimotopes), protease inhibitor 100x (Roche), forward and reverse GFP primers (Sigma Genosys), bicinchoninic acid (BCA) protein assay kit (Pierce), and ECL plus Western Blotting Detection System was purchased from GE Healthcare. Antiglyceraldehyde-3-phosphate dehydrogenase (GAPDH; clone 6C5) antibody (AbCam Ltd.), GFP Rabbit Antibody (Cell Signaling Technology), polyclonal goat antimouse immunoglobulin/HRP and polyclonal goat antirabbit immunoglobulin/HRP were obtained from Dako.

Instruments. *Nuclear Magnetic Resonance (NMR) Spectroscopy.* ^{1}H NMR spectra were measured using a Bruker DPX 300 MHz spectrometer. Deuterated water (D_2O; Cambridge Isotope Laboratories) was used as the solvent for solution state NMR analyses.

Gel Permeation Chromatography. Gel permeation chromatography (GPC) was performed using *N*,*N*-dimethylacetamide (DMAc; 0.03% w/v LiBr, 0.05% w/v 2,6-dibutyl-4-methylphenol (BHT); Sigma-Aldrich) as the mobile phase. Polymer solutions (3−5 mg/mL in

dx.doi.org/10.1021/bm4013088 | *Biomacromolecules* 2013, 14, 4135−4149

DMAc) were injected into GPC at 40 °C (flow rate =1 mL/min). A Shimadzu modular system comprising an SIL-10AD autoinjector, a PL 5.0-mm bead-size guard column (50 mm × 7.8 mm) followed by four linear PL (Styragel) columns (10^5, 10^4, 10^3, and 100 Å) was used. Calibration was achieved with commercial polystyrene standards ranging from 500 to 10^6 g/mol. The calibration curve, acquired by the Mark−Houwink equation, was utilized for determining the relative molecular weight of polymers by relating their retention time (in same mobile phase) to the molecular weight of the reference standards.

Dynamic Light Scattering. Dynamic light-scattering (DLS) studies and ζ-potential measurements were performed using a Malvern Zetasizer NaNo ZS Instrument (Malvern, USA) equipped with a 4 mV He-Ne laser operating at λ = 633 nm, an avalanche photodiode detector with high quantum efficiency, and an ALV/LSE-5003 multiple tau digital correlator electronics system. Size measurements were performed in Disposable Solvent Resistant Micro Cuvettes ZEN0040 (Malvern Instruments) recorded in nanometers (nm) while charge readings were conducted in Folded Capillary Cells DTS1060 (Malvern Instruments) shown in millivolts (mV). The polyplex solutions were prepared with appropriate buffers where particle concentrations of 0.25 mg/mL DNA (for P(MAA-*co*-CMA) series) and 15 μM of siRNA (for Q-P(DMAEMA-*co*-CMA) series) were employed. Size and stability measurements were conducted at 37 °C, while surface charge investigations were performed at 25 °C. All samples were measured by scanning seven times with each time of automatic measurement. Size and ζ analyses were performed in triplicates while stability measurements were conducted in duplicates.

Methods. *Cell Culture and Toxicity.* Human neuroblastoma SHEP cells, human liver hepatocellular carcinoma (HepG2) cells, human non-small-cell lung cancer (NSCLC) H460 cells, and human fetal lung fibroblast (MRC5) cells were utilized to assess polymer toxicity. H460 cells were grown in Roswell Park Memorial Institute (RPMI) medium with HEPES and L-glutamine, while SHEP, HepG2 and MRC5 cell lines were grown in Dulbecco's Modified Eagle Medium (DMEM) containing 4.5 g/L glucose and L-glutamine, both media were supplemented with 10% Fetal Calf Serum (FCS). All cells were cultured at 37 °C in a 95% humidified atmosphere of 5% CO_2. For the cell viability assay, cells were seeded in 96-well sterile flat-bottom plates (appropriate number of cells needed for each well was determined from growth curves) and incubated for 24 h to ensure adherence. Upon surface attachment cells were treated with polymer solutions at varying concentrations and were further incubated for 72 h. After the incubation period, 20 μL of AlamarBlue[32] was added to each well, and incubated for another 6 h. Absorbance was measured by a Benchmark Plus Microplate Spectrophotometer at 570 nm. The percentage of viability was expressed as a function of positive control cells (cells only in media) representing 100% viability. The treatments were done with five replicates and the assay was independently repeated three times.

Polyelectrolyte Complex Formation and Characterization. The gene binding ability of both P(MAA-*co*-CMA) and Q-P(DMAEMA-*co*-CMA) copolymer series was evaluated by agarose gel electrophoresis. P(MAA-*co*-CMA)/DNA complexes were formed on the basis of electrostatic interactions between oligolysine (amine; N), DNA (phosphate; P) and P(MAA-*co*-CMA) (carboxylate; C). The charge ratio (wt %) between P(MAA-*co*-CMA) and DNA was set to 1:1 (C/P; 50 ng) in PBS (0.01 M), and the N ratio was altered from 0.5 to 50 (25 ng to 2.5 μg oligolysine) throughout the study. Particle preparation included complexing the oligolysine to DNA (50 ng, 2 μL) first incubating for 15 min then adding P(MAA-*co*-CMA) (50 ng, 5 μL) to the mixture and incubating further for 15 min with continuous shaking on a rotary shaker. The total volume of ternary samples was made up to 15 μL using PBS. Q-P(DMAEMA-*co*-CMA)/siRNA complexes with varying N/P ratios were prepared spontaneously in pH 5.0 buffer (0.01 M) solutions. Particles were formulated according to the mole ratio between amine (Q-P(DMAEMA-*co*-CMA)) and phosphate (siRNA) groups where they were incubated for 30 min. 0.8% and 2% agarose gels containing GelRed Nucleic Acid Stain 10,000× in water (Biotium) were casted prior to electrophoresis to investigate DNA and siRNA complexation, respectively. 2.5 μL of 5x DNA Loading Buffer, Blue (BioLine), was added to each sample before they were loaded on to the gel. As reference points, a ladder (HyperLadder II or EasyLadder II (Bioline)), a naked gene sample, and a naked polymer sample were included in the gel. Electrophoresis took place in Tris-borate-EDTA (TBE) buffer (BioRad), for 1.5 h at 80 V and 1 h at 60 V for DNA and siRNA conjugation studies, respectively. Complete complexation was visualized by a BioRad UV Transilluminator (model No: Universal Hood II) and imaged with a Quantity One Gel Doc XR software program. Particle size, stability and charge studies were performed on a Malvern Zetasizer NaNo ZS Instrument.

Gene Transfection. To investigate the transfection efficiency of polymers, DNA and siRNA complexes were formulated and delivered into SHEP and green fluorescent protein (GFP)-expressing SHEP cells (GFP-SHEP), respectively. GFP-SHEP cells were maintained in antibiotic-treated DMEM (Geneticin 14 μL/mL) medium complemented with 10% FCS. Antibiotic treatments were removed and replaced with fresh media before performing experiments on the GFP-expressing cell lines. SHEP cells were seeded in 6-well plates (100×10^3 cells/well for SHEP; 60×10^3 cells/well for GFP-SHEP) and incubated for 24 h prior to the treatments. Transfection media (Opti-MEM) comprising the polymers and their conjugated therapeutics were prepared at various N/P ratios and concentrations. One hour after complex formation, treatments were added into the plates and seeded with cells for 5 h. As reference points were positive controls: gene complexes prepared with a commercially available transfection agent Lipofectamine 2000 (L2K), along with negative control experiments: Opti-MEM only, gene only, and L2K only (mock-transfected) were included. After 5 h the transfection medium was replaced with DMEM (10% FCS) media and further incubated for 48−72 h (depending on the analysis technique) at 37 °C in 5% CO_2 and 95% humidity. GFP mRNA, protein and fluorescence intensity levels were assessed using real-time quantitative PCR (RT-qPCR), Western blotting, and flow cytometry (FACSCanto; Becton-Dickinson).

GFP mRNA Analysis via Real-Time Quantitative PCR. Expression of GFP mRNA in GFP-SHEP cells was examined using RT-qPCR. Total RNA isolations were performed as previously described.[33,34] The RT-qPCR was performed using the Applied Biosystems high-capacity cDNA reverse transcription and SYBR green kits. Data was normalized to the house keeping gene, β2-microglobulin (β2M), by coamplifying both sequences in the same reaction and analyzing their real-time PCR amplification using the ABI PRISM 7900 Sequence Detection System (Applied Biosystems). The gene-specific primers employed for PCR amplification are listed in Supporting Information (Table S2). All experiments were conducted in triplicate.

GFP Protein Analysis via Western Blotting. Cellular protein was isolated from cell pellets by solubilizing on ice in radio-immunoprecipitation assay (RIPA) buffer containing protease inhibitors. Equal amounts of protein (10 μg) were loaded onto freshly prepared 10% SDS-PAGE gels and transferred to nitrocellulose membranes. Protein expression of GFP and loading control GAPDH were determined as previously described.[34] The experiments were repeated in triplicate with protein isolated from three independent extractions.

Fluorescence Microscopy Imaging. SHEP cells (5000−7000 cells/dish) were plated in 35 mm cultured dishes which were precoated with DBL poly-D-lysine hydrobromide (Sigma) for 5 min. After 72 h of surface adherence, cells were transfected with either P(MAA-co-CMA)-oligolysine-TUBB-pREP4 plasmid complexes or Q-P(DMAEMA-*co*-CMA)-AlexaFlour488 conjugated siRNA complexes for 5 h at 37 °C. Transfected cells were rinsed with PBS and then stained with the appropriate nuclear dye; 5 μM DRAQ5 (Cell Signaling Technology) or 5 μg/mL bisBenzimide H 33342 trihydrochloride (Hoescht 33342, Sigma-Aldrich) for 5 min. Two types of confocal microscopes, Zeiss LSM 780 and Leica TCS SP5, were used to capture the images. Controls included fluorescently tagged genes alone, genes complexed to L2K, and Opti-MEM treated samples.

RESULTS AND DISCUSSION

Determination of Cell Viability via AlamarBlue Assay. AlamarBlue cell viability assay was employed to determine the toxicity profile of the cholesterol-derived ionic copolymers on

dx.doi.org/10.1021/bm4013088 | *Biomacromolecules* 2013, 14, 4135−4149

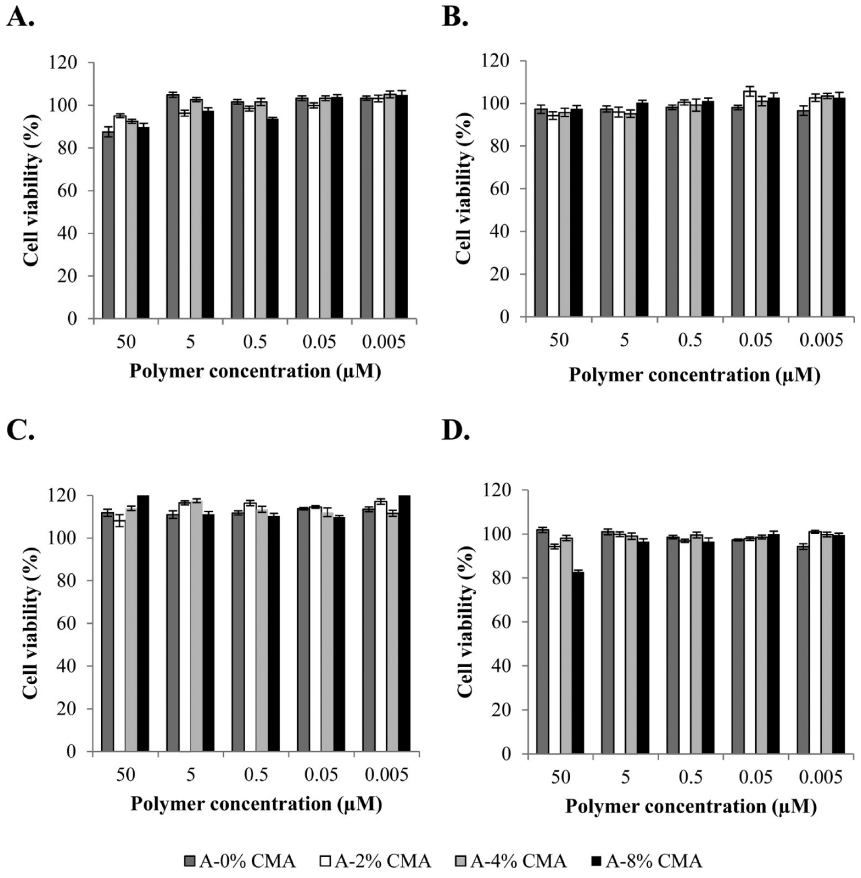

Figure 1. Viability of (A) human neuroblastoma (SHEP) cells, (B) human liver hepatocellular carcinoma (HepG2) cells, (C) human lung cancer (H460) cells, and (D) normal human fetal lung (MRC5) cells after incubation with P(MAA-*co*-CMA) copolymers of A-2% CMA, A-4% CMA, and A-8% CMA along with P(MAA) (A-0% CMA) for 72 h, measured with AlamarBlue assay. The assay was repeated three times in five replicates, and the viability results were normalized according to the positive control (untreated cells). Error bars represent standard deviation ($P < 0.05$).

various human cell lines. The assay is based on the ability of metabolically active cells to convert the redox dye resazurin into the end product, resorufin, which is easily detected via fluorescence or absorbance spectrophotometric readers.[35] The viability of SHEP, HepG2, H460 and MRC5 cells was assessed as a function of P(MAA-*co*-CMA) (Figure 1) and Q-P(DMAEMA-*co*-CMA) (Figure 2) treatments at varying concentrations (0.005−50 μM).

Overall the anionic copolymers (A-2% CMA, A-4% CMA, A-8% CMA, and P(MAA)) demonstrated lower toxicity results than those reported for poly-L-lysine (10000 g/mol,[36] 12000 g/mol,[37] 25000 g/mol[38]) in HepG2 and A2780 carcinoma cell lines. The viability of the cells for 50 μM to 0.05 μM treatments varied between 86% and 100%, indicating that these copolymers display no major toxicity, which is in agreement with previous reports regarding anionic polymer toxicity.[8,12,39] The half-maximal inhibitory concentration (IC_{50}) doses of the anionic copolymers were not calculated due to their exceptionally low toxicity values in the concentration range studied.

In comparison to the anionic copolymers, between 50 μM and 0.05 μM treatments, Q-P(DMAEMA-*co*-CMA) copolymer series displayed higher levels of cytotoxicity owing to their cationic nature. Polymer treatments below 5 μM concentration displayed toxicity results comparable with those of various other cationic polymers.[26,37] As anticipated, the incorporation of hydrophobic moieties (for Q-15% CMA and Q-20% CMA) reduced the toxicity effect of the copolymers at higher concentrations (5 μM) in HepG2 and H460 carcinoma cell lines. The IC_{50} values of Q-P(DMAEMA-*co*-CMA) copolymer series illustrated in Table S3 (Supporting Information), suggest that compositions with 2%, 4%, and 8% CMA units display higher IC_{50} values than those reported for commercially available jetPEI (0.3 to 1.3 μM in HeLa cells).[40] Q-P(DMAEMA-*co*-CMA) formulations with 15% and 20% CMA showed IC_{50} values of 5.0 and 9.0 μM in HepG2 cells and 2.9 and 6.0 μM in H460 cells, respectively. The overall toxicity profile of this library permits further *in vitro* studies to be conducted in these cell lines.

Formation of Polyelectrolyte Complexes. The library of CMA-derived ionic copolymers was utilized to form stable polyplexes with nucleic acids via electrostatic interactions (Scheme 1). Agarose gel electrophoresis was employed to determine the complete conjugation ratios of both P(MAA-*co*-CMA) (weight ratio) and Q-P(DMAEMA-*co*-CMA) (molar ratio) based complexes. The strong anionic nature of P(MAA-*co*-CMA) series prohibited complexation with negatively charged nucleic acids. Therefore, a cationic linker, oligolysine, was introduced into the mixture to form stable delivery complexes that integrated both of the negatively charged components. Oligolysine, a short chain lysine polymer with 10 repeating units, was selected due to its efficient condensing ability to nucleotides and its low toxicity profile.[41] In addition to playing a pivotal role in assembling the entire complex, oligolysine could *possibly* increase the overall transfection efficiency of the complex.[42,43]

An initial study was conducted on condensing oligolysine to siRNA; however, low electrostatic binding between the two components, due to siRNA size and oligolysine surface charge,[44] resulted in incomplete complexation (Figure S2, Supporting

dx.doi.org/10.1021/bm4013088 | *Biomacromolecules* 2013, 14, 4135−4149

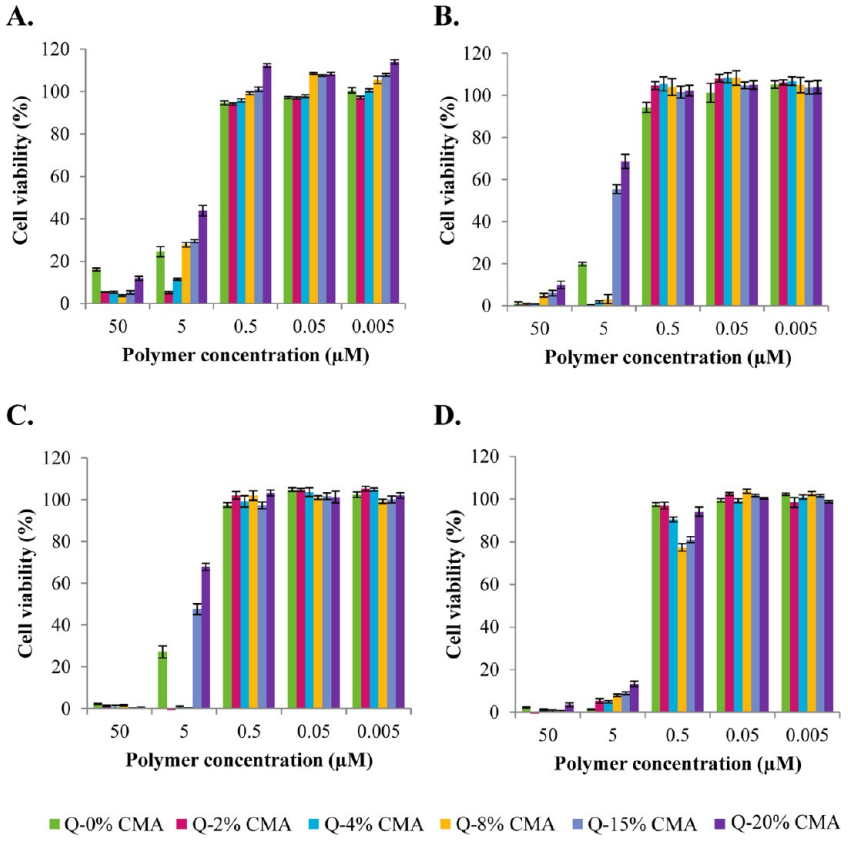

Figure 2. Viability of (A) human neuroblastoma (SHEP) cells, (B) human liver hepatocellular carcinoma (HepG2) cells, (C) human lung cancer (H460) cells and (D) normal human fetal lung (MRC5) cells after incubation with Q-P(DMAEMA-*co*-CMA) copolymers that consist of 2%, 4%, 8%, 15% and 20% CMA along with Q-P(DMAEMA) (Q-0% CMA) for 72 h, measured with Alamar Blue assay. The assay was repeated three times in five replicates, and the viability results were normalized according to the positive control (untreated cells). Error bars represent standard deviation ($P < 0.05$).

Information). Alternatively, DNA (13.1 kb) was utilized for ternary complexation assays. Binary complexes formed between the positive rich domains of oligolysine and negatively charged phosphate backbones of DNA, were prepared at N/P ratios ranging from 0.5:1 to 4:1, each complex corresponding to 50 ng DNA (Figure S3, Supporting Information). Complete retardation (absence of naked DNA bands) was observed in lanes 7−10, indicating binary complexation N/P ratios to be 1.5:1 and over. Ternary complexes were formed by fixing the phosphate/carboxylate (P/C) ratio of DNA to P(MAA-*co*-CMA) at 1:1 (50 ng), while increasing the amine ratio (N) of oligolysine from 0.5 to 50 (25 ng to 2.5 μg) (Figure 3A). It was predicted that increasing the amine groups in the complex would intensify the interactions among the binary complex and P(MAA-*co*-CMA); therefore exhibit complexation ratios higher than 1.5:1 (binary complexation).[45] Overall stable polyelectrolyte complexes incorporating DNA and oligolysine were formed with N/P/C ratios of 4:1:1, 4:1:1, and 6:1:1 for A-2% CMA, A-4% CMA and A-8% CMA, respectively. The higher complexation ratio, seen in A-8% CMA, is due to the higher amount of cholesterol groups hindering the carboxylic acid groups and obstructing their ionic interactions with the amine units (of oligolysine), thus driving the complexation ratio to higher N/P/C values to achieve full conjugation.

Q-P(DMAEMA-*co*-CMA)-siRNA polyelectrolyte complex formation was based on spontaneous electrostatic interactions between the cationic amine units (present in the cationic polymer) and anionic phosphate groups (seen on the siRNA phosphate backbone). A representative gel is shown in Figure 3B where Q-20% CMA is conjugated to siRNA (5 pmol; phosphate molar ratio fixed at 1) at varying N/P ratios from 2:1 to 30:1. Complete gel retardation (absence of free siRNA bands) for Q-20% CMA-siRNA was achieved at 8:1 and above. With increasing amounts of amine units (decreasing CMA moieties), the mobility of siRNA retarded at lower N/P ratios resulting from either size change in the complex, neutralization of the anionic groups or simpler complexation in the absence of hindrance caused by CMA units.[46] The siRNA complexation ratios for Q-2% CMA, Q-4% CMA, Q-8% CMA, Q-15% CMA and Q-20% CMA copolymers were revealed as 4:1, 6:1, 6:1, 6:1 and 8:1 respectively, which are comparable results to previous DMAEMA reports.[23,47,48] The decreasing amount of protonable amine groups in the polymer composition, from Q-2% CMA to Q-20% CMA, drove the complexation ratios to slightly higher N/P values in order to attain complete conjugation.

Overall gel electrophoresis illustrated the minimum charge ratios necessary for full complexation of P(MAA-*co*-CMA)-oligolysine-DNA and Q-P(DMAEMA-*co*-CMA)-siRNA conjugate series. However, the ideal N/P ratios, which demonstrate the greatest transfection efficiency and lowest cell toxicity, tend to be higher than the minimum charge ratio.[3,47] Preliminary studies, conducted via flow cytometry, revealed the optimal N/P ratios for ternary complexes [(P(MAA-*co*-CMA)-oligolysine-DNA) and Q-P(DMAEMA-*co*-CMA)-siRNA complex series] to range between 6:1:1 to 50:1:1, and 20:1 to 150:1, respectively.

Characterization of Polyelectrolyte Complexes: Size, Surface Charge, and Stability Analysis. Transfection

Scheme 1. Formation of (A) P(MAA-*co*-CMA)-oligolysine-DNA Ternary Complexes and (B) Q-P(DMAEMA-*co*-CMA)-siRNA Binary Complexes

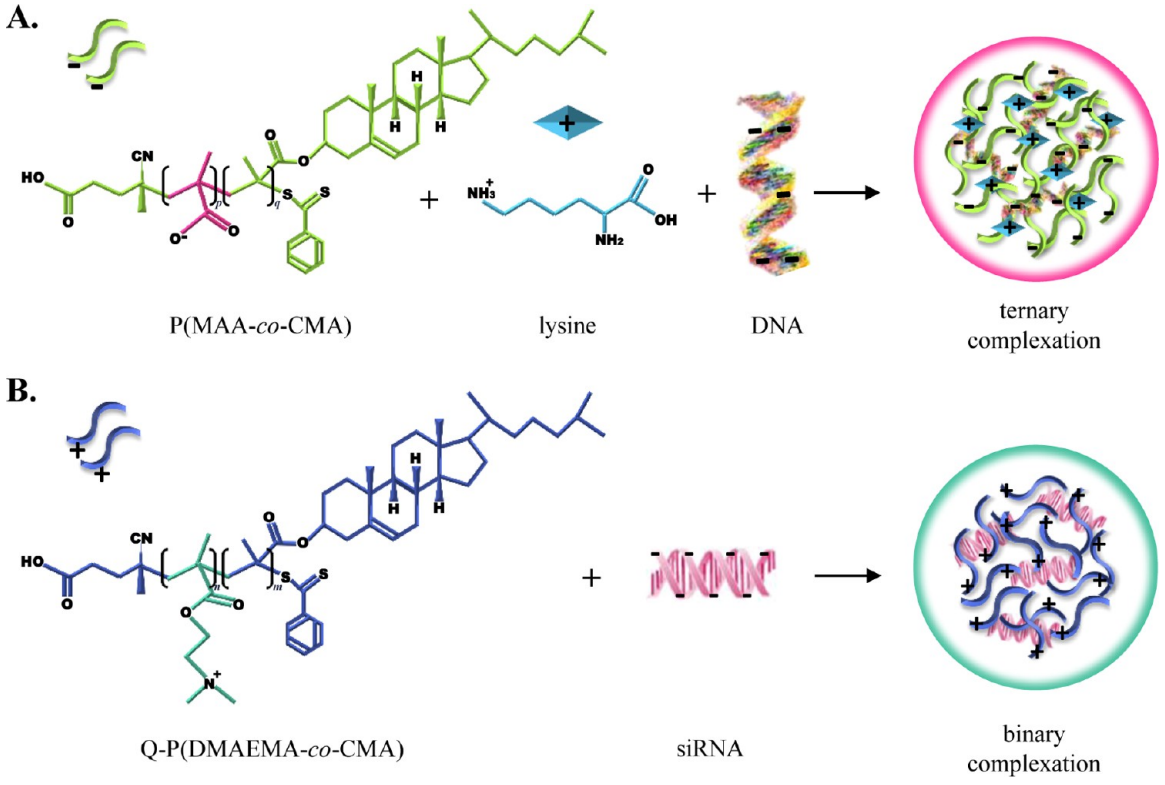

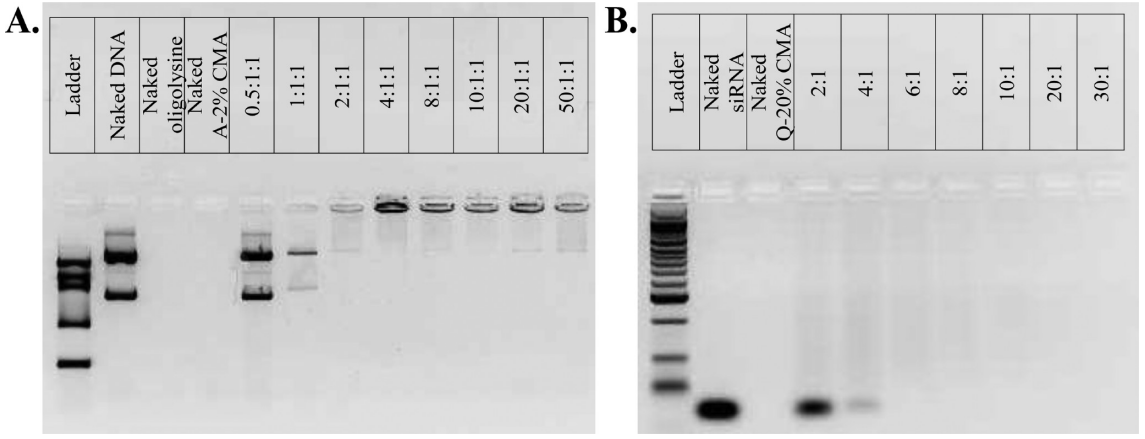

Figure 3. Agarose gel electrophoresis of (A) oligolysine/DNA/A-2% CMA polymer complexes (B) Q-20% CMA polymer: siRNA conjugates prepared at varying amine/phosphate/carboxylate (N/P/C) ratios and N/P ratios, respectively. (A) 0.8% Agarose gel: Lane 1: EasyLadder II, Lane 2: Naked DNA, Lane 3: Naked oligolysine, Lane 4: Naked A-2% CMA, Lanes 5−12: ternary complexes at N/P/C ratios from 0.5:1:1 to 50:1:1. (B) 2% Agarose gel: Lane 1: HyperLadder II, Lane 2: Naked siRNA, Lane 3: Naked Q-20% CMA, Lanes 4−10: binary conjugates at N/P ratios of 2:1 to 30:1.

efficiency is strongly influenced by properties such as polyplex size and ζ potential.[49] Accordingly, P(MAA-*co*-CMA)-oligolysine-DNA and Q-P(DMAEMA-*co*-CMA)-siRNA complexes were characterized for their particle size, surface charge and hydrodynamic stability via dynamic light scattering.

Prior to P(MAA-*co*-CMA)-oligolysine-DNA ternary complex investigations, binary complexes (oligolysine-DNA) prepared at N/P ratios of 6:1, 12:1 and 50:1 were analyzed for their mean diameters (Figure S4A, Supporting Information) Earlier studies conducted on oligolysine-DNA condensation revealed the existence of a 'critical oligolysine concentration' which represents the minimum amount of oligolysine necessary for creating stable complexes. Above the 'critical concentration' threshold (>6:1) the light scattering intensity of the complexes remained constant resulting in similar hydrodynamic diameters, as seen in Supporting Information, Figure S4A (54.2 ± 2.6 nm (N/P 6:1), 60.2 ± 2.0 nm (N/P 12:1), 60.7 ± 1.8 nm (N/P 50:1)).[50] Nevertheless, the addition of P(MAA-*co*-CMA) copolymers enhanced the overall size of the ternary complexes from 60.2 ± 5.6 nm to 69.4 ± 2.6 for A-2% CMA, 75.7 ± 0.6 nm to 91.6 ± 2.3 nm for A-4% CMA and 82.1 ± 2.2 nm to 94.6 ± 1.5 nm for A-8% CMA with increasing amine conjugation ratios (Table 1). Complexes prepared with A-2% CMA, displayed a more compact structure owing its complexation behavior being mostly driven

dx.doi.org/10.1021/bm4013088 | *Biomacromolecules* 2013, 14, 4135−4149

Table 1. Size and ζ-Potential Measurements of P(MAA-*co*-CMA)-oligolysine-DNA Complexes at Varying N/P/C Ratios

N/P/C ratio	polymer composition	diameter (nm)	ζ-potential (mV)
6:1:1	A-2% CMA	60.2 ± 5.6	22.3 ± 0.9
	A-4% CMA	75.7 ± 0.6	21.7 ± 0.3
	A-8% CMA	82.1 ± 2.2	32.3 ± 1.1
12:1:1	A-2% CMA	62.6 ± 2.3	23.1 ± 1.9
	A-4% CMA	74.5 ± 1.1	30.7 ± 1.1
	A-8% CMA	82.9 ± 2.1	38.2 ± 0.7
50:1:1	A-2% CMA	69.4 ± 2.6	27.9 ± 1.6
	A-4% CMA	91.6 ± 2.3	30.8 ± 1.5
	A-8% CMA	94.6 ± 1.5	37.2 ± 1.0

by the methacrylic acid subunits. While A-8% CMA complexes formed bigger molecules as its conjugation was influence by bulky, cholesterol subunits.

Ternary complexes prepared with P(MAA-*co*-CMA) copolymer series exhibited a similar zeta potential pattern where complexes of 6:1:1, 12:1:1 and 50:1:1 N/P/C ratios were all positively charged (Table 1 and Figure S4B, Supporting Information). Complexes with overall cationic charge are more susceptible to cellular internalization owing to their attraction toward the negatively charged plasma membrane.[22,51] The zeta potential of A-2% CMA complexes displayed charge values of 22.3 mV (6:1:1), 23.1 mV (12:1:1) and 27.9 mV (50:1:1). This increase in zeta potential can be attributed to the addition of amine units (from 6 to 50) in the final complex. Charge values for complexes of A-4% CMA and A-8% CMA displayed the same trend; ranging from 21.8 mV to 30.8 mV and 32.3 mV to 37.2 mV, respectively. The differences in the intensity of zeta potential between P(MAA-*co*-CMA) series is credited to the organization of the copolymers in solution state. Copolymer compositions with increasing CMA units tend to form supramolecular structures, where lipid moieties are brought together exposing the charged molecules on the outer layer.[31] Additionally, with decreasing MAA moieties in the copolymer composition, fewer acidic groups occupy the oligolysine amine units triggering the complexes to exhibit *overall* higher surface charges.

Table 2 represents the diameter and ζ-potential of Q-P(DMAEMA-*co*-CMA)-siRNA complexes prepared at N/P

Table 2. Size and ζ-Potential Measurements of Q-P(DMAEMA-*co*-CMA)-siRNA Complexes at N/P Ratio of 20:1

polymer composition	diameter (nm)	ζ-potential (mV)
Q-2% CMA	41.7 ± 4.8	64.4 ± 0.8
Q-4% CMA	45.8 ± 2.1	60.6 ± 0.9
Q-8% CMA	51.9 ± 1.7	51.0 ± 1.3
Q-15% CMA	57.0 ± 3.4	46.1 ± 1.4
Q-20% CMA	72.5 ± 3.7	48.9 ± 1.2

20:1 ratio in aqueous solution. The effective diameter of complexes increased from 41.7 ± 4.8 nm to 72.5 ± 3.7 nm as the CMA ratio changed from 2 to 20%. Concurring with previous findings[52] and P(MAA-*co*-CMA)-oligolysine-DNA ternary complexes, the particle size of Q-P(DMAEMA-*co*-CMA) gene vectors increased proportionally with the bulky hydrophobic cholesterol content in the copolymers, ensuing Q-20% CMA-siRNA complexes to exhibit the largest size at N/P 20:1 ratio. The ζ-potential of Q-P(DMAEMA-*co*-CMA)-siRNA complex series (20:1) showed a slight reduction with increasing cholesterol units (decreasing DMAEMA entities) once again verifying the charge influence of the amine content and the shielding effect of CMA moieties on the copolymer.[53]

Increasing the cationic density of complexes typically enhances the cellular uptake and gene transfection efficiency.[51,54] Thus complexes with higher N/P ratios (>20:1) were prepared to examine the change in their size and ζ properties. Polyelectrolyte formation with copolymers comprising Q-2%, Q-4% and Q-8% CMA (high amine content), at N/P ratios greater than 20:1, enhanced the cationic charge density of the particle but was predicted to promote toxicity (in line with IC_{50} values). In contrast, Q-15% and Q-20% CMA copolymers (with lower surface charge) required higher amounts of polymers per nucleic acid condensation thus permitting complexation ratios up to 150:1 to be utilized without causing severe toxicity. Consequently representative Q-20% CMA-siRNA polyplexes were further examined with N/P ratios ranging from 50:1 to 150:1 in Table 3.

Table 3. Size and ζ-Potential Measurements of Q-20% CMA-siRNA Complexes at Varying N/P Ratios

N/P ratios	diameter (nm)	ζ-potential (mV)
Q-20% CMA (50:1)	54.4 ± 1.7	55.6 ± 1.2
Q-20% CMA (100:1)	51.2 ± 1.4	58.1 ± 1.6
Q-20% CMA (150:1)	49.3 ± 2.4	59.7 ± 1.2

The complex diameters decreased with increasing complexation N/P ratios owing to the enhancement in charge ratios which elevated the electrostatic forces between polyelectrolyte and siRNA. The cationic ζ-potential of Q-20% CMA-siRNA polyplexes at 50:1 N/P ratios showed a slim increase in comparison to N/P 150:1.

Complexes, which are formed on the basis of electrostatic interactions, have the tendency to shrink, aggregate and/or produce larger supramolecular structures progressively with time.[55] P(MAA-*co*-CMA)-oligolysine-DNA complexes formed at N/P/C ratios of at 6:1:1 displayed similar diameters, among each P(MAA-*co*-CMA) series, throughout time portraying characteristics of stable particles (Figure 4A). Moreover, polyelectrolyte complexes of 12:1:1 (N/P/C ratio) illustrated a steady trend in the first hour; however, fluctuations in the 90th minute resulted in minor decreases in the hydrodynamic diameters (Figure 4B). With the highest conjugation ratio of 50:1:1 ternary complexes revealed size enlargement within the hour (Figure 4C). Over time the complexes formed unstable aggregates with reducing diameters; which was expected as highly charged cationic polyplexes are quite susceptible to collapse and form unstable particles in aqueous suspensions.[56] *PDI* data (Table S4, Supporting Information) obtained from DLS verify the stability of complexes prepared at 6:1:1 and 12:1:1 ratio along with the unsteadiness of 50:1:1 complexes overtime.

The stability profile of Q-P(DMAEMA-*co*-CMA)-siRNA series at varying complexation ratios were examined in OptiMeM within 20 min intervals for 2 h (Figure 5). Polyelectrolyte complexes formed at N/P ratios of 20:1 exhibited a steady trend overtime with minimal fluctuations (±8.4 nm) in their hydrodynamic diameter overall portraying features of stable particles (Figure 5A). At higher N/P ratios Q-20% CMA-siRNA complexes formed particles smaller particles which demonstrated steady diameters for the first 80 to 100 min.

In summary, results indicate that the hydrodynamic diameter and zeta potential of the polyplexes are immensely influenced by the CMA ratio in the polymer composition (increasing in size with increasing CMA units) and the quantity of charge species

dx.doi.org/10.1021/bm4013088 | *Biomacromolecules* 2013, 14, 4135−4149

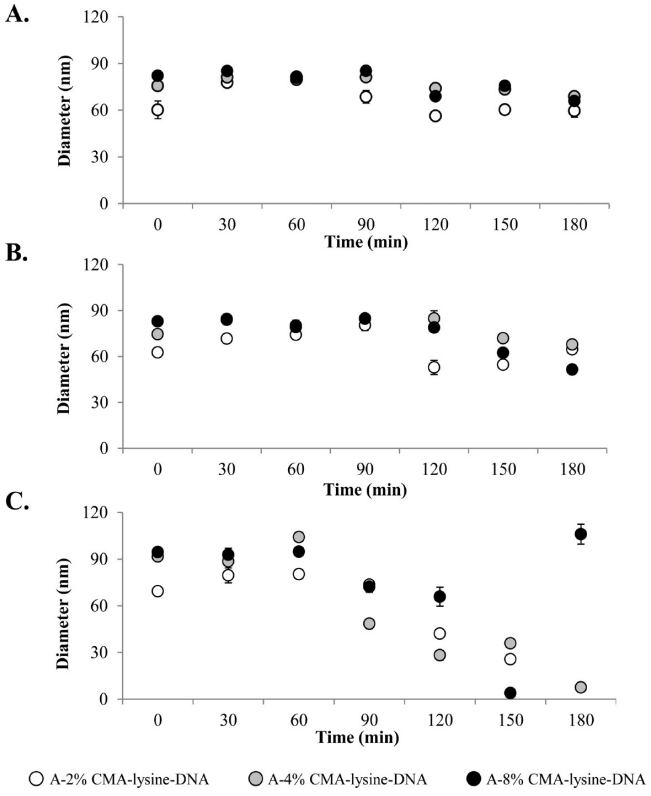

Figure 4. The hydrodynamic stability of P(MAA-*co*-CMA)-oligolysine-DNA complexes, in terms of aggregate formation, determined by dynamic light scattering as a function of time. The diameter of complexes prepared at N/P/C ratios of (A) 6:1:1, (B) 12:1:1 and (C) 50:1:1 in PBS (pH 7.4) at 37 °C.

covering the complex surface (increasing charge with increasing protonable amines). Owing to their efficient size (<100 nm) and cationic surface charge, P(MAA-*co*-CMA)-oligolysine-DNA and Q-P(DMAEMA-*co*-CMA)-siRNA complex series are both plausible candidates for overcoming cellular barriers and effectively entering cells.[57] However, fluctuations in P(MAA-*co*-CMA)-oligolysine-DNA complexes stability, diminishes their use in *in vivo* therapy. Conversely the stability profile of Q-P(DMAEMA-*co*-CMA)-siRNA polyplexes offers the siRNA a longer *in vivo* half-life than free siRNA component, as siRNA would degrade instantly in its free form.[58] Stable polyplexes like these, with diameters less than 100 nm, are plausible candidates for passive tumor targeting via the enhanced permeability and retention (EPR) effect.[59−61] The EPR effect relies on enhanced vascular permeability and reduced lymphatic drainage of capillaries surrounding the tumors which trigger the accumulation of macromolecules to the tumor sites.[58,59] Accordingly, untargeted stable complexes are more susceptible to bypass the healthy tissues, as they would be easily removed by lymphatic drainage, and gather in the pathological sites affected with leaky vasculature (like inflammation and tumor areas) and enhance therapeutic delivery to those sites.[62] Overall the compact size, high cationic nature and stability profile of these Q-P(DMAEMA-*co*-CMA)-siRNA polyplexes hold potential for enhancing therapeutic delivery in *in vivo* cancer cells.

***In vitro* Gene Transfection Studies.** The transfection efficacy of P(MAA-*co*-CMA)-oligolysine-DNA and Q-P(DMAEMA-*co*-CMA)-GFP siRNA complexes were evaluated via various analysis techniques (RT-qPCR, western, flow cytometry) in SHEP and GFP expressing SHEP cells, respectively.

SHEP cells transfected with P(MAA-*co*-CMA)-oligolysine-DNA complexes prepared with GFP expressing (pmaxFP-GreenC) plasmids (2 μg/mL) for 72 h were analyzed by Western blotting and flow cytometry for GFP protein quantification and fluorescence intensity, respectively. Post-72 h treatments protein extracts were gathered from samples and quantified by western analysis. The protein of interest, GFP, along with the house keeping protein, GAPDH, bands were distinguished with suitable antibodies, and measured by densitometry relative to SHEP control (Figure 6A). Figure 6B displays the relative GFP protein expression (%) attained by ternary complexes which were prepared at various N/P/C ratios. P(MAA-*co*-CMA)-oligolysine-DNA complexes demonstrated no more than 14% GFP protein expression where the expression reduced with increasing amine (N) charge ratio. DNA transfection via L2K displayed 1.7-folds higher GFP expression than the ternary complexes in SHEP cells. The ternary complexes transfection efficiency determined by flow cytometry - showing <2.5% GFP fluorescence intensity - is portrayed in Figure 6C in comparison to L2K-DNA control. This discrepancy in results can be attributed the difference between the two analysis techniques, as one is quantifying protein (stable throughout measurements) and the other is measuring fluorescence (may vary upon absorbing light).

The ternary complexes, with increasing oligolysine units, displayed very low gene transfection efficacy in both protein and fluorescence intensity levels. In line with gel retardation assays; lysine polymers, one of the first cationic polymers used for gene transfection,[63] have shown efficient binding to DNA and enhanced protection against nuclease degradation.[64] However, lysine polymers are prone to demonstrate nominal transfection ability when applied alone, as they cannot facilitate or induce endosomal release of DNA.[65] Ternary systems were designed with P(MAA-*co*-CMA) moieties in order to induce membrane destabilization and overcome the setbacks associated with oligolysine delivery. Although increased amounts of oligolysine (overall cationic charge) may occupy the majority of the anionic groups (associated to P(MAA-*co*-CMA)) thus prevent membrane interactions from taking place. High levels of lysine molecules overpower the P(MAA-*co*-CMA) units, obscuring their membrane disruptive properties, ultimately causing the system to perform as a binary-complex of oligolysine-DNA instead; which is a system notorious for exhibiting nominal transfection efficacy.[55] In the case of protein quantification, results suggested that increasing amine conjugation ratios from (6:1:1) to (50:1:1) reduced the transfection efficiency from roughly 14% to 4.5%. This can be attributed to the greater surface charge triggering stronger electrostatic interactions with DNA molecules, the formation of unstable aggregates (in line with stability studies), and relative toxicity.[66]

In vitro transfection activity of Q-P(DMAEMA-*co*-CMA)-siRNA complexes were evaluated in GFP-SHEP cells utilizing anti-GFP siRNA (50 nM) against the gene of interest. Prior to transfection assays; a time-lapse study (at 24, 48, 72, 96, 120 h) was undertaken to evaluate the knockdown efficiency of the anti-GFP siRNA sequence in GFP-SHEP cells using L2K (Figures S5−S7, Supporting Information). The siRNA transfection activity, examined at two different concentrations 50 nM and 100 nM, revealed the maximal levels of GFP knockdown to occur at 48 h (for mRNA knockdown) and 72 h (for protein and fluorescence intensity suppression) time points. Accordingly the gene silencing efficiency of polyplexes, mRNA expression levels in GFP-SHEP cells were analyzed via RT-qPCR analysis at 48 h post-siRNA transfection. Gene level suppression observed in GFP-SHEP cells was highly

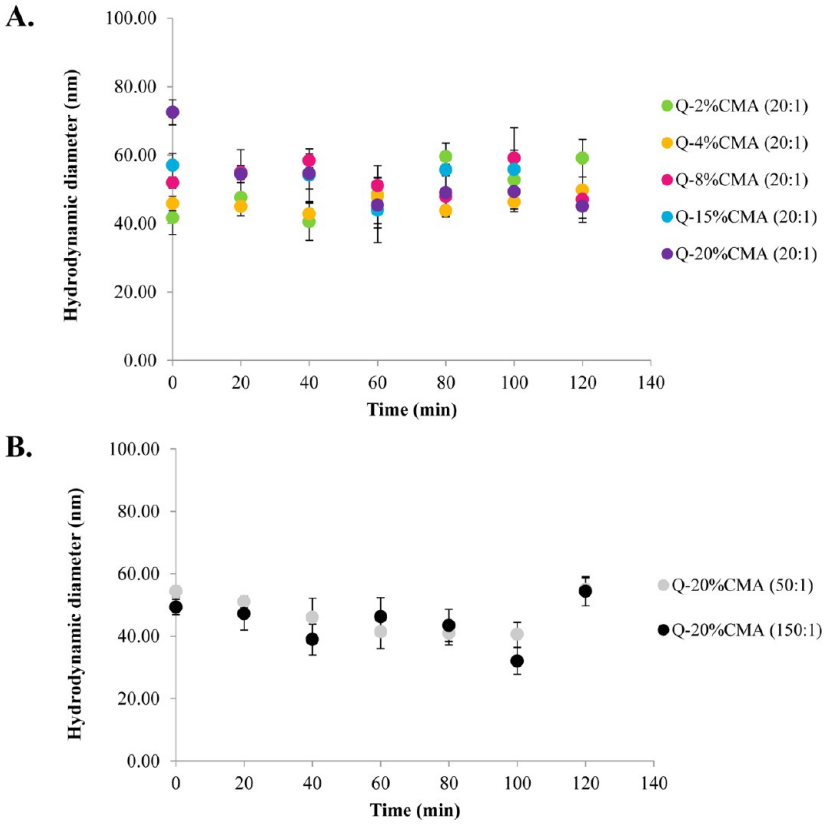

Figure 5. Hydrodynamic stability of Q-P(DMAEMA-*co*-CMA)-siRNA complexes. Polyplex diameters were analyzed in OptiMeM by dynamic light scattering as a function of time. (A) Q-P(DMAEMA-*co*-CMA)-siRNA complex series with an N/P ratio of 20:1 (Q-0% CMA as 0% (20:1), Q-2% CMA as 2% (20:1), Q-4% CMA as 4% (20:1), Q-8% CMA as 8% (20:1), Q-15% CMA as 15% (20:1), Q-20% CMA as 20% (20:1)) (B) representative Q-20% CMA-siRNA conjugates prepared at N/P ratios of 50:1 and 150:1 ((20% (50:1) and 20% (150:1)).

dependent on polymer composition and the polyplex N/P ratio. Copolymers comprising higher amine groups displayed greater transfection efficiency at low N/P ratios (20:1) and higher rates of toxicity at N/P 50:1 and over (Figure 7A,B). Copolymers with low buffering capacity; Q-15% CMA and Q-20% CMA entailed higher doses of polymers in their complex formulation ($N \geq 50$), to promote endosomal escape under the influence of the proton sponge effect and further advance their transfection activity.[67] Q-20% CMA-siRNA polyplexes prepared at N/P ratio 150:1 demonstrated the greatest gene silencing profile, in its series, owing to its increased surface charge which promoted higher buffering capacity therefore greater endo/lysosomal rupture. The delicate balance between the hydrophobic and hydrophilic components of the polymer design allows Q-20%CMA-siRNA polyplexes to be formed at N/P ratios as high as 150:1 without projecting any toxicity toward the cells.[54]

The protein level inhibition achieved by Q-P(DMAEMA-*co*-CMA)-siRNA complexes at varying N/P ratios for 72 h, are illustrated in Figure 7C,D. The time lag between mRNA and protein silencing is correlated to the half-lives of both components, particularly the half-life of the proteins being longer than its corresponding transcript.[68] Similar to gene knockdown studies, at these N/P 20:1 ratio, copolymers with higher DMAEMA ratios demonstrated greater transfection efficiency. Of the complexes, the highest protein knockdown was achieved by copolymer Q-2% CMA (82.2%) having suppression levels similar to L2K-siRNA (94.6%) and Q-P(DMAEMA)-siRNA (90.0%) complexes. Upon increasing the N/P conjugation ratio to 50:1, copolymers Q-15% CMA and Q-20% CMA displayed higher transfection profiles. The efficacy of Q-15% CMA increased by 1.8-folds when complexed at N/P 50:1; whereas Q-20% CMA-siRNA complexes multiplied their protein knockdown efficiency at N/P ratios 50:1 and over. The enhancement in polyplex transfection activity is likely due to the increase in particle zeta potential which enforces higher degrees of cellular binding and consequently greater transfection.[3,69] On the other hand Q-P(DMAEMA)-siRNA (Q-0% CMA) polyplexes prepared at N/P ratios higher than 50:1 exhibited high toxicity (verified throughout imaging, protein and gene quantification experiments), once again validating the significance of CMA integration to the polymer chain. Cholesterol introduces benefits by improving biocompatibility, facilitating intracellular dissociation (by causing steric hindrance and triggering less compact binding to payload) and assisting in membrane interactions.[54] Cholesterol-based systems have been utilized in a number for studies for siRNA delivery both *in vitro*[51,70] and *in vivo*.[54,71] Cationic lipid-based constructs are the most established systems used for the systemic delivery of siRNA into the liver.[72] The liver comprises numerous siRNA targets such as hepatitis, fibrosis, hepatocellular carcinoma and cholesterol biosynthesis.[73] Thus, studies investigating siRNA activity via cholesterol based-systems have shown promising results in hepatocellular carcinoma cells HepG2 and Huh-7 *in vitro*.[71,74] In accordance with cell viability results—polymers illustrating higher IC_{50} values in HepG2 cells—Q-(DMAEMA-*co*-CMA) copolymer series are more likely to exhibit higher levels of siRNA transfection if they were to be analyzed in hepatocellular carcinoma cells.

Figure 7E,F illustrates the fluorescence intensity suppression 72 h after Q-P(PMAEMA-*co*-CMA)-siRNA transfection in GFP-SHEP cells. All copolymers exhibited reasonable activity

dx.doi.org/10.1021/bm4013088 | *Biomacromolecules* 2013, 14, 4135−4149

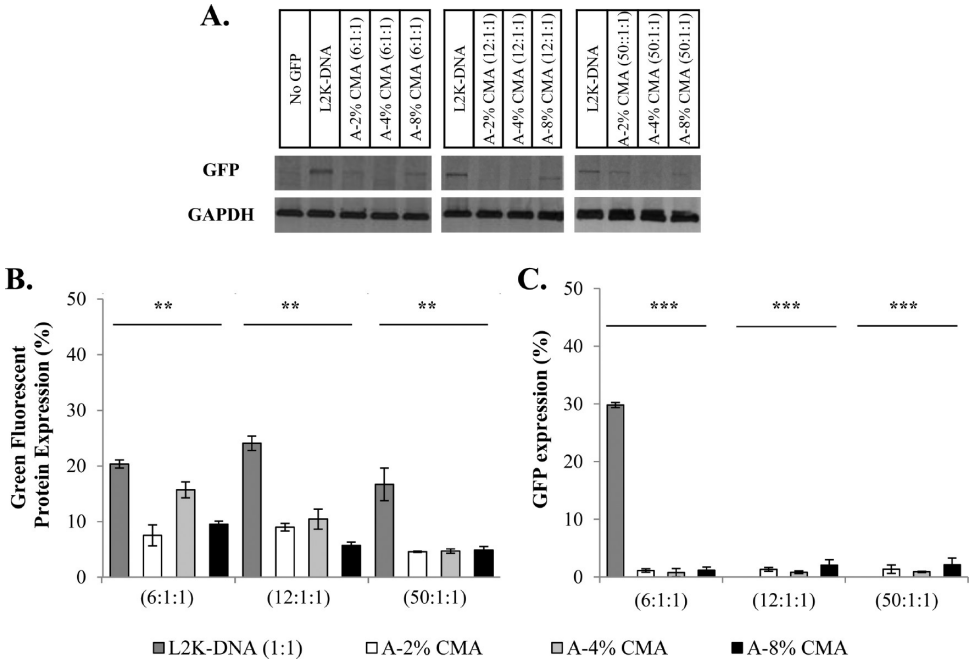

Figure 6. Transfection efficiency of polyelectrolyte complexes *in vitro* evaluation in SHEP cells (A) Representative immunoblot image of the post-72 h P(MAA-*co*-CMA)-oligolysine-DNA (2 μg/mL DNA) transfection study. Upper band: GFP; lower band: GAPDH loading control. (B) Graphical illustration of the quantitative analysis of relative GFP protein expression normalized to GAPDH loading control using untreated L2K-DNA cells as the reference. (C) GFP fluorescence intensity expression results determined by flow cytometry of SHEP cells at 72 h post transfection with P(MAA-*co*-CMA)-oligolysine-DNA complex series. Treatments include 2 μg/mL DNA delivery by L2K (positive control) and P(MAA-*co*-CMA)-oligolysine-DNA complex series with N/P/C ratios of 6:1:1, 12:1:1 and 50:1:1. Controls comprise of untreated SHEP cells and L2K only treatments for 72 h. The data represents the mean ± SD of three independent experiments (**P < 0.005, ***P < 0.0005 versus L2K-DNA).

in transfecting siRNA; however, highest suppression levels were achieved by Q-2% CMA (70.0% GFP knockdown). The transfection efficiency of copolymers at N/P ratio 20:1 followed the order of Q-2% CMA (70.0%) > Q-4% CMA (68.4%) > Q-8% CMA (63.0%) > Q-15% CMA (53.3%) > Q-20% CMA (35.9%). The gradual decrease in transfection activity can be accounted for by the increasing cholesterol units, in the copolymer composition, which are known to shield the surface charge and cause steric hindrance.[69] Particle shielding counteracts interactions with the cell surface and as a result can hinder the cellular uptake process and reduce the transfection efficacy of the therapeutic complex.[53,75] Furthermore, copolymers with decreasing DMAEMA units (tertiary amine groups) display weaker siRNA binding that may cause complex dissociation prior to cell internalization and thus exhibit lower levels of gene silencing.[53] The optimal transfection activity mediated by Q-2% CMA (20:1) was comparable to the gene silencing levels of both Q-P(DMAEMA) (Q-0% CMA) and L2K. Q-2% CMA-siRNA complexes achieved higher transfection values at N/P ratio of 20:1 in comparison to the widely used control transfection regent; branched-poly-(ethyleneimine) (bPEI)[25,76](25000 g/mol) employed in MDA-MB-435-GFP (human breast cancer cell line), NIH 3T3 (fibroblast cell line) and Neuro-2a (murine neuroblastoma cell line), respectively. The representative histogram of flow cytometry for Q-P(DMAEMA-*co*-CMA)-siRNA (20:1) series treatments is shown in Figure S8, Supporting Information. The plot illustrates GFP suppression in GFP-SHEP cells with a distinct shift to the left; moving further away from the control with higher transfection efficiency with decreasing cholesterol content. To achieve higher levels of transfection, the N/P ratios of Q-P(DMAEMA-*co*-CMA)-siRNA conjugates were increased to 50:1, 100:1 and 150:1. With increasing amine ratios complexes comprised higher levels of free cationic DMAEMA groups that altered the viability and transfection efficiency of the cells.[67] While Q-2% CMA, Q-4% CMA, and Q-8% CMA showed significant toxicity, Q-15% CMA and Q-20% CMA demonstrated adequate results. The transfection efficiency of Q-20% CMA was enhanced from 35.9% to 44.2% at the N/P ratio of 50:1 due to an increase in charge density, electrostatic interactions and ultimately siRNA condensation.[25,47] The fluorescence intensity, protein and gene knockdown profiles of Q-20%CMA-siRNA complexes, prepared with $N \geq 50$ amine ratios, overall demonstrate efficient siRNA silencing without inducing significant levels of toxicity. Due to nontoxic effects and enhanced stability Q-20%CMA-siRNA complexes ($N/P \geq 50:1$), which are P(DMAEMA)-derived polyplexes well-known for their long circulating properties,[69] these systems have potential *in vivo* applications.

Cellular Uptake Imaging Studies. The cellular distribution profile of P(MAA-*co*-CMA)-oligolysine-DNA and Q-P(DMAEMA-*co*-CMA)-siRNA complex series was investigated in SHEP cells by confocal laser scanning microscopy (CLSM). L2K mediated gene delivery illustrated in Figure S9A, Supporting Information and Figure 8A was identified as positive control-images for SHEP cells; due to the efficient gene delivery properties of L2K based systems which exhibit reasonable levels of DNA uptake and localize siRNA molecules in the cytoplasm.[77]

Ternary complexes comprising oligolysine, TUBB-pREP4 plasmid DNA (no fluorescence) and Alexa Fluor 488 labeled A-8% CMA (green) copolymers were prepared at varying N/P/C ratios (6:1:1, 12:1:1, 50:1:1) and incubated in cells for 5 h prior to imaging. Alexa Fluor 488 labeled A-8% CMA was generated by tailoring small amounts of carboxylic molecules on the copolymer into stable amide bonds that carry reactive dithiols via EDC/sulfo-NHS reactions[78] and labeling them with a

dx.doi.org/10.1021/bm4013088 | *Biomacromolecules* 2013, 14, 4135−4149

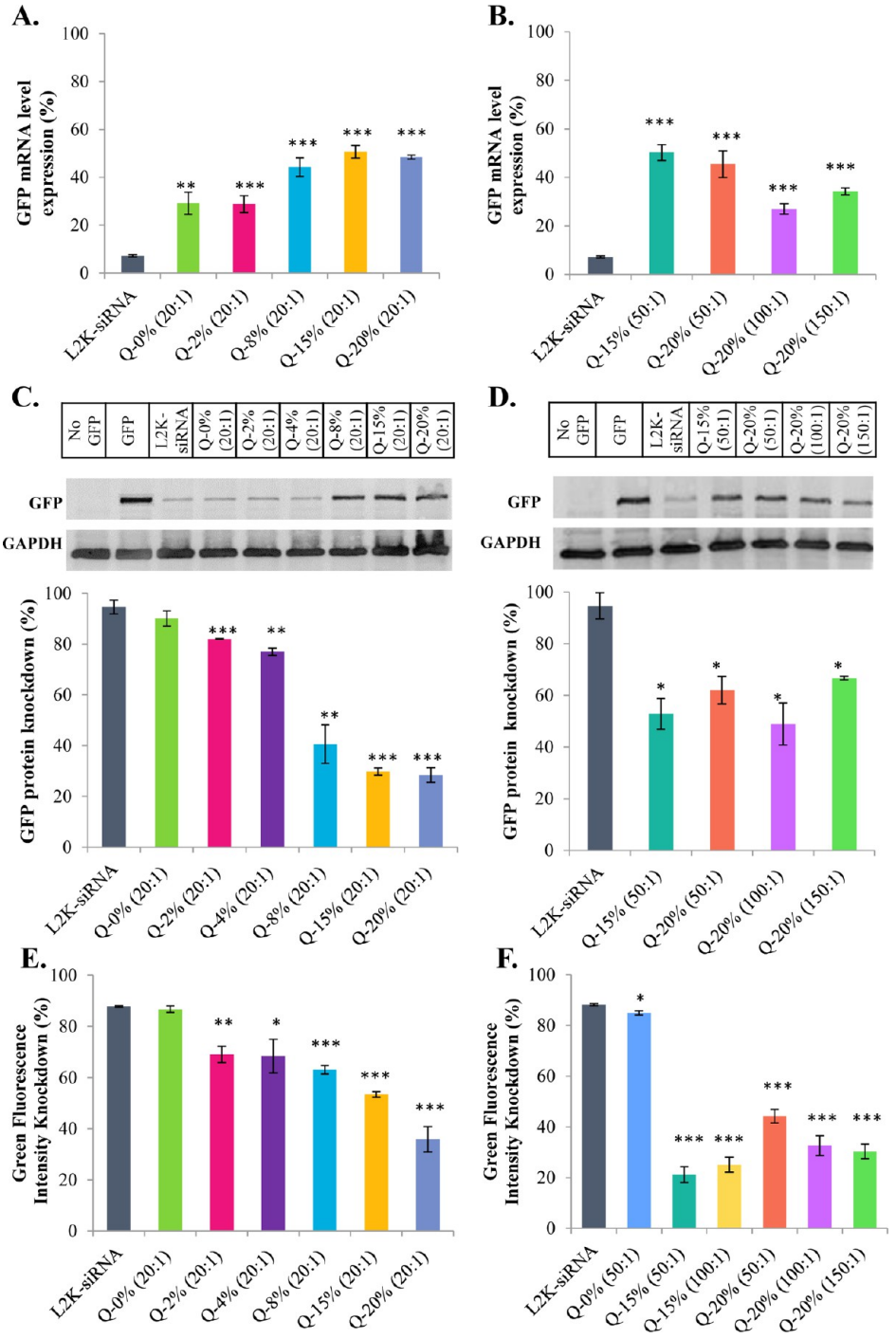

Figure 7. Transfection efficiency of Q-P(DMAEMA-*co*-CMA)-siRNA complexes in GFP-SHEP cells with 50 nM anti-GFP siRNA at varying N/P ratios. Analysis of GFP mRNA expression by RT-qPCR following 48 h treatments of (A) L2K-siRNA (positive control) and Q-P(DMAEMA-*co*-CMA)-siRNA polyplex series at N/P 20:1 ratio (Q-0% CMA-siRNA as Q-0% (20:1), Q-2% CMA-siRNA as Q-2% (20:1), Q-4% CMA-siRNA as Q-4% (20:1), Q-8% CMA-siRNA as Q-8% (20:1), Q-15% CMA-siRNA as Q-15% (20:1), Q-20% CMA-siRNA as Q-20% (20:1)). (B) Q-P(DMAEMA-*co*-CMA)-siRNA transfection study comprised of Q-15% CMA-siRNA (N/P ratio 50:1 as Q-15% (50:1)) and Q-20% CMA (N/P ratios of 50:1, 100:1, 150:1 shown as Q-20% (50:1), Q-20% (100:1), Q-20% (150:1) respectively). All values were normalized to the housekeeping gene β2-microglobulin. GFP protein suppression studies determined by Western blotting post 72 h polyplex treatments. (C) Representative immunoblot image and graphical illustration of the relative GFP protein expression in GFP-SHEP cells after Q-P(DMAEMA-*co*-CMA)-siRNA complex (N/P 20:1) treatments. (D) A representative Western blot for the transfection study of Q-15% CMA-siRNA (N/P ratio 50:1) and Q-20% CMA-siRNA (N/P ratios of 50:1, 100:1, 150:1) followed by the quantitative analysis of GFP protein expression expressed as a normalized ratio to untreated GFP-SHEP cells. Upper band: GFP; lower band: GAPDH loading control. GFP fluorescence intensity inhibition results determined by flow cytometry 72 h post transfection with Q-P(DMAEMA-*co*-CMA) copolymer series at (E) N/P ratios of 20:1, (F) N/P ratios of 50:1 and 100:1 for Q-15% CMA-siRNA (as Q-15% (50:1), Q-15% (100:1)) and N/P ratios of 50:1, 100:1 and 150:1 for Q-20% CMA. Controls comprise of untreated GFP-SHEP cells, L2K only, L2K-siRNA, untreated SHEP cells, and Q-P(DMAEMA-*co*-CMA) series only treatments for 72 h. The data represents the mean ± SD of three to four independent experiments (*$P < 0.05$, **$P < 0.005$, ***$P < 0.0005$ versus L2K-siRNA).

dx.doi.org/10.1021/bm4013088 | *Biomacromolecules* 2013, 14, 4135−4149

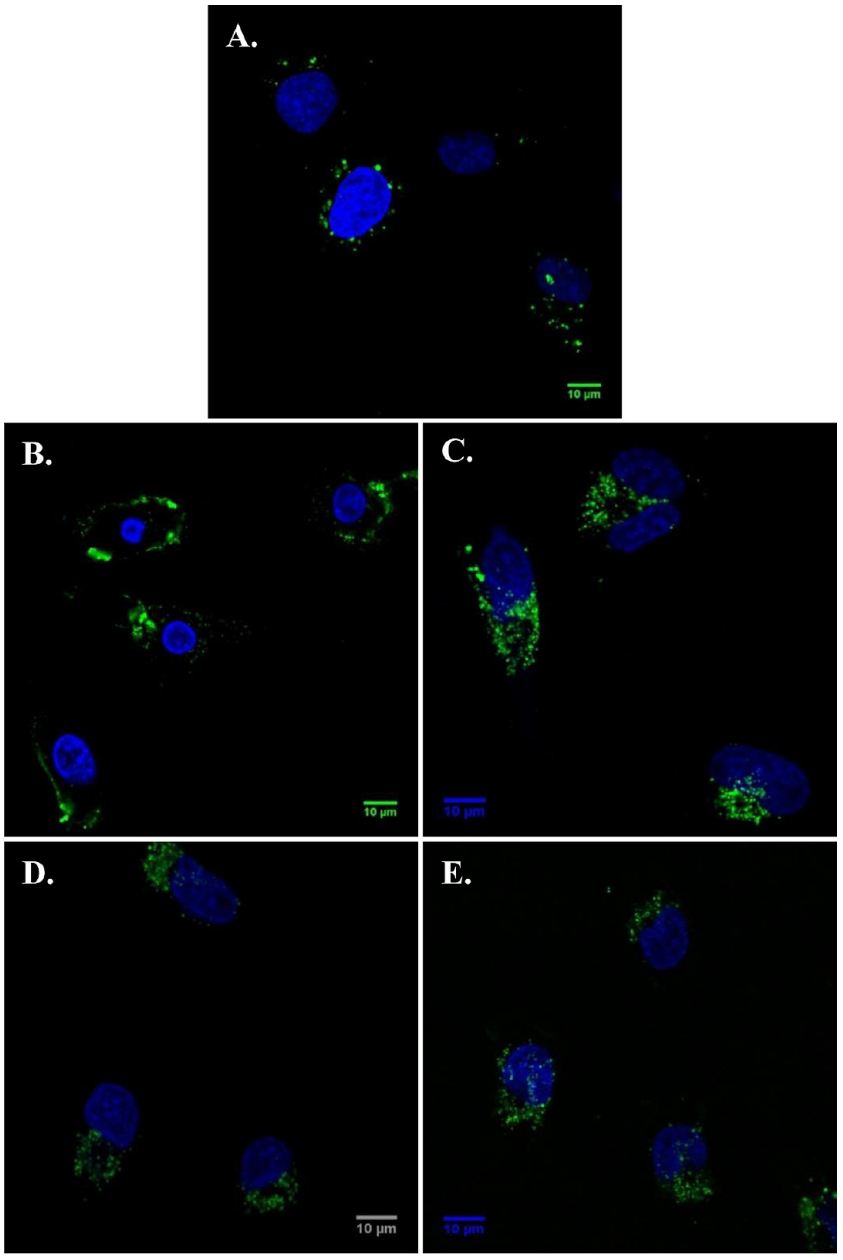

Figure 8. Confocal laser scanning microscopy exhibiting cell uptake of Q-P(DMAEMA-*co*-CMA)-siRNA conjugates in SHEP cells after 5 h of incubation: (A) L2K-siRNA (50 nM) (control); (B) N/P (20:1) Q-2% CMA-siRNA (50 nM siRNA); (C) N/P (50:1) Q-20% CMA-siRNA (50 nM siRNA); (D) N/P (100:1) Q-20% CMA-siRNA (50 nM siRNA); (E) N/P (200:1) Q-20% CMA-siRNA (25 nM siRNA). Nuclei are visualized with Hoechst 33342 stain. Alexa Fluor 488-conjugated siRNA was utilized for the assay, and fluorescent images were acquired at λ_{ex} = 495 nm and λ_{em} = 591 nm. Scale bars correspond to 10 μm.

fluorescent maleimide dye. The Alexa Fluor dye content of the-modified copolymer was found to be 0.22 mol %; which is sufficient for effective detection by flow cytometry and confocal microscopy analysis.[79] Transfected DNA molecules along with the cell nuclei were stained with 5 μM DRAQ5 nuclear dye (magenta). Representative images of Alexa Fluor 488 labeled A-8% CMA-oligolysine-DNA complexes prepared at 6:1:1 (N/P/C ratio) are displayed in Supporting Information, Figure S9B,C for SHEP cells. In line with gel electrophoresis, ternary complexation was similarly confirmed by confocal microscopy, owing to the image layers of DNA molecules (magenta) and Alexa Fluor 488 labeled-copolymers (green) coinciding with each other at identical sites Notably, Alexa Fluor 488 labeled A-8% CMA-oligolysine-DNA complexes formed small aggregates (indicated by arrows) adhering to the cell surface and/or outside the cells. The assembly of aggregates can be contributed to depletion of stability observed in complexes over time (in agreement with DLS studies).[48] While a few conjugates were internalized (indicated by blue arrows) at 6:1:1 ratio, ternary complexes prepared at higher conjugation ratios (50:1:1; larger aggregates) were merely stuck on the cell surface owing to their enhanced surface charge (Figure S9 (D-E), Supporting Information).

A control study investigating the cellular uptake profile of binary complexes -comprising oligolysine and Alexa Fluor 488 labeled A-8% CMA- resulted in small aggregates and adhered to the surface of the cells (Figure S10, Supporting Information). The interactions between binary complexes and cells were

dx.doi.org/10.1021/bm4013088 | *Biomacromolecules* 2013, 14, 4135−4149

governed by nonspecific ionic interactions between the positive complex and negatively charged cell surface. Lysine polyplexes are usually equipped with ligands that facilitate cell uptake and endosomal escape.[80] However, the ionic interactions overpowered the predicted hydrophobic interactions (between the membrane and P(MAA-*co*-CMA) copolymers), resulting in systems with only binding ability rather than cell internalization capability.

Representative images of Q-P(DMAEMA-*co*-CMA) copolymers (Q-2% CMA and Q-20% CMA) delivering 50 nM Alexa Fluor 488 conjugated siRNA are shown in Figure 8 B,C. Strong fluorescence signals were observed in the cytoplasm with Q-2% CMA-siRNA complexes at their optimal N/P ratio 20:1. Trials runs with Q-2% CMA-siRNA polyplexes at higher conjugation ratios resulted in images of cells in distress due to the increased number of unoccupied positive charges (free DMAEMA units) which are prone to cause cell death.[48,81]

Q-20% CMA-siRNA polyplexes at N/P ratio of 50:1 uniformly distributed siRNA throughout the cellular cytoplasm revealing high transfection efficiency. Q-20% CMA-siRNA complexes prepared with higher conjugation ratios (100:1 and 200:1) demonstrated efficient internalization of siRNA to the cytoplasm (Figure 8D,E). DMAEMA polymers tend to act as proton sponges in endosomal pH, the tertiary amine groups trigger a transition in their conformation which evidently raptures the endosome.[21,82] Overall images revealed that siRNA was well dispersed in the cytoplasm and in line with their high transfection efficiency indicating polyplex treatments successfully escaped the endosomes.

In summary, the cell uptake profile of P(MAA-*co*-CMA)-oligolysine-DNA and Q-P(DMAEMA-*co*-CMA)-siRNA complex series demonstrated differing end-results. The delivery issues -associated with Alexa Fluor 488 labeled A-8% CMA-oligolysine-DNA ternary systems- elucidated by confocal microscopy were consistent to those observed in the GFP transfection studies. Their efficiency was limited due to the system favoring ionic interactions, which facilitate strong binding to negatively charged membrane surfaces, over interactions through cholesterol units that can facilitate internalization. Ultimately, this kind of behavior enforces interactions with charged serum proteins in the circulation system and resulting in negligible gene delivery levels, increased toxicity and rapid clearance from the body.[81] One possible method to inhibit aggregation and unwanted interactions with *in vivo* serum components would be to integrate stable biocompatible PEG molecules to the complex that could reduce the challenging intramolecular interactions.[37,83] Suitably, cell uptake results, consistent with the gene knockdown studies, revealed that Q-P(DMAEMA-*co*-CMA) copolymers are vastly more effective at internalizing genes, escaping the endosomal-lysosomal pathway and releasing their cargo (aka siRNA) into the cytoplasm.

CONCLUSION

In conclusion, a library of CMA-derived ionic copolymers composed of both biological and synthetic moieties with diverse surface charges were evaluated for their therapeutic efficiency. The cholesterol units in the copolymer composition were altered to carefully tune the physicochemical properties and functions of the biohybrid constructs. As predicted, incorporating cholesterol entities into the cationic polymer chains reduced the overall toxicity (in H460 and HepG2 cell lines), whereas in anionic systems there was no significant toxicity regardless of CMA. Therapeutic complexes (for siRNA and DNA) were prepared purely on the basis of electrostatic interactions, resulting in P(MAA-*co*-CMA)-oligolysine-DNA and Q-(P(DMAEMA-*co*-CMA)-siRNA complexes at complexation ratios starting from 6:1:1 (N/P/C) and 20:1 (N/P), respectively. The hydrodynamic diameter, ζ potential and complex stability were evaluated in accord with conjugation ratios and mol % of cholesterol (present in the polymer composition). The therapeutic efficiency of the polyplexes was assessed in SHEP cells via transfection and imaging assays, illuminating the positive and negative attributes of each therapeutic design. In the case of anionic copolymers, ternary complexes exhibited hurdles with gene delivery and were alternatively used for drug delivery applications (future work). The increasing cholesterol content throughout the Q-P(DMAEMA-*co*-CMA) copolymer series enhanced the biocompatibility of the polyplexes (by reducing toxicity with increasing CMA units in the composition), prompted their membrane interactions, and enabled their intracellular dissociation. The hydrophobic anchors also improved the stability of the cationic copolymers in physiological conditions, ultimately leading to an increase in the circulation time. Similar to *in vivo*-jetPEI, cationic linear polymers instantly interacted with their therapeutics (siRNA), forming positively charged polyplexes that were efficiently internalized, while avoiding cargo degradation (via proton sponge effect). The gene delivery (siRNA silencing) profile of Q-P(DMAEMA-*co*-CMA)-siRNA complexes, reported herein, suggests that these positively charged, stable particles are promising candidates for further *in vivo* investigations.

ASSOCIATED CONTENT

Supporting Information

Experimental method for the quaternization of P(DMAEMA-*co*-CMA) copolymers, IC_{50} values of Q-P(DMAEMA-*co*-CMA) copolymer series, and a FACS analysis histogram of GFP-SHEP cells treated with Q-P(DMAEMA-*co*-CMA)-siRNA polyplexes. Hydrodynamic diameters, ζ-potentials, polydispersities, and cellular uptake images of ternary complexes (P(MAA-*co*-CMA)-oligolysine-DNA), agarose gel electrophoresis of oligolysine-siRNA and oligolysine-DNA binary complexes, confocal images of P(MAA-*co*-CMA)-oligolysine binary complexes, primers used for PCR amplification, and a time-lapse GFP knockdown study of L2K-siRNA transfection in GFP-SHEP cells; Figures S1−S10, Tables S1−S4. This material is available free of charge via the Internet at http://pubs.acs.org.

AUTHOR INFORMATION

Corresponding Authors

*Telephone: +90 232 7506660. E-mail: volgabulmus@iyte.edu.tr.
*Telephone: +61 2 93854371. E-mail: Thomas.p.davis@monash.edu).

Notes

The authors declare no competing financial interest.

ACKNOWLEDGMENTS

We acknowledge the Australian Research Council (ARC) for funding (DP 0770818).

REFERENCES

(1) Roth, J. A.; Cristiano, R. J. *J. Natl. Cancer Inst.* **1997**, *89* (1), 21−39.
(2) Reid, T.; Galanis, E.; Abbruzzese, J.; Sze, D.; Andrews, J.; Romel, L.; Hatfield, M.; Rubin, J.; Kirn, D. *Gene Ther.* **2001**, *8* (21), 1618−1626.
(3) Zhang, Y.; Zheng, M.; Kissel, T.; Agarwal, S. *Biomacromolecules* **2011**, *13* (2), 313−322.
(4) Everts, M.; Saini, V.; Leddon, J. L.; Kok, R. J.; Stoff-Khalili, M.; Preuss, M. A.; Millican, C. L.; Perkins, G.; Brown, J. M.; Bagaria, H.;

Nikles, D. E.; Johnson, D. T.; Zharov, V. P.; Curiel, D. T. *Nano Lett.* **2006**, *6* (4), 587−591.
(5) Kimchi-Sarfaty, C.; Brittain, S.; Garfield, S.; Caplen, N. J.; Tang, Q.; Gottesman, M. M. *Hum. Gene Ther.* **2005**, *16* (9), 1110−1115.
(6) Boyer, C.; Bulmus, V.; Davis, T. P.; Ladmiral, V.; Liu, J. Q.; Perrier, S. *Chem. Rev.* **2009**, *109* (11), 5402−5436.
(7) Pissuwan, D.; Boyer, C.; Gunasekaran, K.; Davis, T. P.; Bulmus, V. *Biomacromolecules* **2010**, *11* (2), 412−420.
(8) Bulmus, V.; Woodward, M.; Lin, L.; Murthy, N.; Stayton, P.; Hoffman, A. *J. Controlled Release* **2003**, *93* (2), 105−120.
(9) Murthy, N.; Robichaud, J. R.; Tirrell, D. A.; Stayton, P. S.; Hoffman, A. S. *J. Controlled Release* **1999**, *61* (1−2), 137−143.
(10) Bulmus, V. *Aust. J. Chem.* **2005**, *58* (6), 411−422.
(11) Borden, K. A.; Eum, K. M.; Langley, K. H.; Tirrell, D. A. *Macromolecules* **1987**, *20* (2), 454−456.
(12) Murthy, N.; Campbell, J.; Fausto, N.; Hoffman, A. S.; Stayton, P. S. *J. Controlled Release* **2003**, *89* (3), 365−374.
(13) Murthy, N.; Chang, I.; Stayton, P.; Hoffman, A. *Macromol. Symp.* **2001**, *172* (1), 49−56.
(14) Lackey, C. A.; Murthy, N.; Press, O. W.; Tirrell, D. A.; Hoffman, A. S.; Stayton, P. S. *Bioconjugate Chem.* **1999**, *10* (3), 401−405.
(15) Lackey, C. A.; Press, O. W.; Hoffman, A. S.; Stayton, P. S. *Abstr. Pap. ACS* **2001**, *221*, U425−U425.
(16) Linhardt, J. G.; Thomas, J. L.; Tirrell, D. A. *Macromolecules* **1999**, *32* (13), 4457−4459.
(17) Ladavière, C.; Tribet, C.; Cribier, S. *Langmuir* **2002**, *18* (20), 7320−7327.
(18) Sanjoh, M.; Miyata, K.; Christie, R. J.; Ishii, T.; Maeda, Y.; Pittella, F.; Hiki, S.; Nishiyama, N.; Kataoka, K. *Biomacromolecules* **2012**, *13* (11), 3641−3649.
(19) Sanjoh, M.; Hiki, S.; Lee, Y.; Oba, M.; Miyata, K.; Ishii, T.; Kataoka, K. *Macromol. Rapid Commun.* **2010**, *31* (13), 1181−1186.
(20) Wang, C.; Luo, X.; Zhao, Y.; Han, L.; Zeng, X.; Feng, M.; Pan, S.; Peng, H.; Wu, C. *Acta Biomater.* **2012**, *8* (8), 3014−3026.
(21) Boussif, O.; LezoualC'H, F.; Zanta, M. A.; Mergny, M. D.; Scherman, D.; Demeneix, B.; Behr, J. P. *Proc. Natl. Acad. Sci. U.S.A.* **1995**, *92* (16), 7297−7301.
(22) Whitehead, K. A.; Langer, R.; Anderson, D. G. *Nat. Rev. Drug Discovery* **2009**, *8* (2), 129−138.
(23) Gary, D. J.; Lee, H.; Sharma, R.; Lee, J.-S.; Kim, Y.; Cui, Z. Y.; Jia, D.; Bowman, V. D.; Chipman, P. R.; Wan, L.; Zou, Y.; Mao, G.; Park, K.; Herbert, B.-S.; Konieczny, S. F.; Won, Y.-Y. *ACS Nano* **2011**, 3493−3505.
(24) Dash, P. R.; Read, M. L.; Barrett, L. B.; Wolfert, M. A.; Seymoura, L. W. *Gene Ther.* **1999**, *6* (4), 643−650.
(25) Zhu, C. H.; Jung, S.; Luo, S. B.; Meng, F. H.; Zhu, X. L.; Park, T. G.; Zhong, Z. Y. *Biomaterials* **2010**, *31* (8), 2408−2416.
(26) Wang, Y.; Wang, L. S.; Goh, S. H.; Yang, Y. Y. *Biomacromolecules* **2007**, *8* (3), 1028−1037.
(27) Mishra, S.; Webster, P.; Davis, M. E. *Eur. J. Pharm. Biopharm.* **2004**, *83* (3), 97−111.
(28) Tao, L.; Chou, W. C.; Tan, B. H.; Davis, T. P. *Macromol. Biosci.* **2010**, *10* (6), 632−637.
(29) Tao, L.; Liu, J. Q.; Tan, B. H.; Davis, T. P. *Macromolecules* **2009**, *42* (14), 4960−4962.
(30) Boyer, C.; Teo, J.; Phillips, P.; Erlich, R. B.; Sagnella, S.; Sharbeen, G.; Dwarte, T.; Duong, H. T.; Goldstein, D.; Davis, T. P.; Kavallaris, M.; McCarroll, J. *Mol. Pharm.* **2013**, *10* (6), 2435−2444.
(31) Sevimli, S.; Inci, F.; Zareie, H. M.; Bulmus, V. *Biomacromolecules* **2012**, *13* (10), 3064−3075.
(32) Sevimli, S.; Sagnella, S.; Kavallaris, M.; Bulmus, V.; Davis, T. P. *Polym. Chem.* **2012**, *3* (8), 2057−2069.
(33) McCarroll, J. A.; Gan, P. P.; Liu, M.; Kavallaris, M. *Cancer Res.* **2010**, *70* (12), 4995−5003.
(34) Kow, S. C.; McCarroll, J.; Valade, D.; Boyer, C.; Dwarte, T.; Davis, T. P.; Kavallaris, M.; Bulmus, V. *Biomacromolecules* **2011**, *12* (12), 4301−4310.
(35) Al-Nasiry, S.; Geusens, N.; Hanssens, M.; Luyten, C.; Pijnenborg, R. *Hum. Reprod.* **2007**, *22* (5), 1304−1309.
(36) Deshpande, M. C.; Garnett, M. C.; Vamvakaki, M.; Bailey, L.; Armes, S. P.; Stolnik, S. *J. Controlled Release* **2002**, *81* (1−2), 185−199.
(37) Patil, M. L.; Zhang, M.; Minko, T. *ACS Nano* **2011**, *5* (3), 1877−1887.
(38) Choi, Y. H.; Liu, F.; Kim, J.-S.; Choi, Y. K.; Jong Sang, P.; Kim, S. W. *J. Controlled Release* **1998**, *54* (1), 39−48.
(39) Kusonwiriyawong, C.; van de Wetering, P.; Hubbell, J. A.; Merkle, H. P.; Walter, E. *Eur. J. Pharm. Biopharm.* **2003**, *56* (2), 237−246.
(40) Bertrand, E.; Goncalves, C.; Billiet, L.; Gomez, J. P.; Pichon, C.; Cheradame, H.; Midoux, P.; Guegan, P. *Chem. Commun.* **2011**, *47* (46), 12547−12549.
(41) Golda, A.; Pelisek, J.; Klocke, R.; Engelmann, M. G.; Rolland, P.-H.; Mekkaoui, C.; Nikol, S. *J. Vasc. Res.* **2007**, *44* (4), 273−282.
(42) McKenzie, D. L.; Collard, W. T.; Rice, K. G. *J. Pept. Res.* **1999**, *54* (4), 311−318.
(43) Vijayanathan, V.; Thomas, T.; Thomas, T. J. *Biochemistry* **2002**, *41* (48), 14085−14094.
(44) Gary, D. J.; Puri, N.; Won, Y.-Y. *J. Controlled Release* **2007**, *121* (1−2), 64−73.
(45) Srinivasan, C.; Burgess, D. J. *J. Controlled Release* **2009**, *136* (1), 62−70.
(46) Zhang, C.; Yadava, P.; Hughes, J. *Methods* **2004**, *33* (2), 144−150.
(47) Guo, S. T.; Huang, Y. Y.; Wei, T.; Zhang, W. D.; Wang, W. W.; Lin, D.; Zhang, X.; Kumar, A.; Du, Q. A.; Xing, J. F.; Deng, L. D.; Liang, Z. C.; Wang, P. C.; Dong, A. J.; Liang, X. J. *Biomaterials* **2011**, *32* (3), 879−889.
(48) Guo, S.; Huang, Y.; Zhang, W.; Wang, W.; Wei, T.; Lin, D.; Xing, J.; Deng, L.; Du, Q.; Liang, Z.; Liang, X.-J.; Dong, A. *Biomaterials* **2011**, *32* (18), 4283−4292.
(49) Cherng, J. Y.; vandeWetering, P.; Talsma, H.; Crommelin, D. J. A.; Hennink, W. E. *Pharm. Res.* **1996**, *13* (7), 1038−1042.
(50) Wadhwa, M. S.; Collard, W. T.; Adami, R. C.; McKenzie, D. L.; Rice, K. G. *Bioconjugate Chem.* **1997**, *8* (1), 81−88.
(51) Tseng, Y.-C.; Mozumdar, S.; Huang, L. *Adv. Drug Delivery Rev.* **2009**, *61* (9), 721−731.
(52) Jiang, T. Y.; Wang, Z. Y.; Tang, L. X.; Mo, F. K.; Chen, C. *J. Appl. Polym. Sci.* **2006**, *99* (5), 2702−2709.
(53) Uzgun, S.; Akdemir, O.; Hasenpusch, G.; Maucksch, C.; Golas, M. M.; Sander, B.; Stark, H.; Imker, R.; Lutz, J. F.; Rudolph, C. *Biomacromolecules* **2010**, *11* (1), 39−50.
(54) Incani, V.; Lavasanifar, A.; Uludag, H. *Soft Matter* **2010**, *6* (10), 2124−2138.
(55) Pack, D. W.; Hoffman, A. S.; Pun, S.; Stayton, P. S. *Nat. Rev. Drug Discovery* **2005**, *4* (7), 581−593.
(56) Kasper, J. C.; Schaffert, D.; Ogris, M.; Wagner, E.; Friess, W. *J. Controlled Release* **2011**, *151* (3), 246−255.
(57) Li, W.; Szoka, F. C. *Pharm. Res.* **2007**, *24* (3), 438−449.
(58) York, A. W.; Kirkland, S. E.; McCormick, C. L. *Adv. Drug Delivery Rev.* **2008**, *60* (9), 1018−1036.
(59) Maeda, H.; Wu, J.; Sawa, T.; Matsumura, Y.; Hori, K. *J. Controlled Release* **2000**, *65* (1−2), 271−284.
(60) Schmaljohann, D. *Adv. Drug Delivery Rev.* **2006**, *58* (15), 1655−1670.
(61) Torchilin, V. P. *J. Controlled Release* **2001**, *73* (2−3), 137−172.
(62) Wu, X. L.; Kim, J. H.; Koo, H.; Bae, S. M.; Shin, H.; Kim, M. S.; Lee, B. H.; Park, R. W.; Kim, I. S.; Choi, K.; Kwon, I. C.; Kim, K.; Lee, D. S. *Bioconjugate Chem.* **2010**, *21* (2), 208−213.
(63) Midoux, P.; Breuzard, G.; Gomes, J. P.; Pichon, C. *Curr. Gene Ther.* **2008**, *8*, 335−352.
(64) Benns, J. M.; Choi, J.-S.; Mahato, R. I.; Park, J.-S.; Kim, S. W. *Bioconjugate Chem.* **2000**, *11* (5), 637−645.
(65) Brown, M. D.; Schätzlein, A.; Brownlie, A.; Jack, V.; Wang, W.; Tetley, L.; Gray, A. I.; Uchegbu, I. F. *Bioconjugate Chem.* **2000**, *11* (6), 880−891.
(66) Zhang, S.; Xu, Y.; Wang, B.; Qiao, W.; Liu, D.; Li, Z. *J. Controlled Release* **2004**, *100* (2), 165−180.
(67) Ping, Y. A.; Liu, C. D.; Tang, G. P.; Li, J. S.; Li, J.; Yang, W. T.; Xu, F. J. *Adv. Funct. Mater.* **2010**, *20* (18), 3106−3116.

(68) Friedel, C. C.; Dölken, L.; Ruzsics, Z.; Koszinowski, U. H.; Zimmer, R. *Nucleic Acids Res.* **2009**, *37* (17), e115.
(69) Verbaan, F. J.; Oussoren, C.; Snel, C. J.; Crommelin, D. J. A.; Hennink, W. E.; Storm, G. *J. Gene Med.* **2004**, *6* (1), 64−75.
(70) Ambardekar, V. V.; Han, H.-Y.; Varney, M. L.; Vinogradov, S. V.; Singh, R. K.; Vetro, J. A. *Biomaterials* **2011**, *32* (5), 1404−1411.
(71) Soutschek, J.; Akinc, A.; Bramlage, B.; Charisse, K.; Constien, R.; Donoghue, M.; Elbashir, S.; Geick, A.; Hadwiger, P.; Harborth, J.; John, M.; Kesavan, V.; Lavine, G.; Pandey, R. K.; Racie, T.; Rajeev, K. G.; Rohl, I.; Toudjarska, I.; Wang, G.; Wuschko, S.; Bumcrot, D.; Koteliansky, V.; Limmer, S.; Manoharan, M.; Vornlocher, H.-P. *Nature* **2004**, *432* (7014), 173−178.
(72) Akinc, A.; Zumbuehl, A.; Goldberg, M.; Leshchiner, E. S.; Busini, V.; Hossain, N.; Bacallado, S. A.; Nguyen, D. N.; Fuller, J.; Alvarez, R.; Borodovsky, A.; Borland, T.; Constien, R.; de Fougerolles, A.; Dorkin, J. R.; Narayanannair Jayaprakash, K.; Jayaraman, M.; John, M.; Koteliansky, V.; Manoharan, M.; Nechev, L.; Qin, J.; Racie, T.; Raitcheva, D.; Rajeev, K. G.; Sah, D. W. Y.; Soutschek, J.; Toudjarska, I.; Vornlocher, H.-P.; Zimmermann, T. S.; Langer, R.; Anderson, D. G. *Nat. Biotechnol.* **2008**, *26* (5), 561−569.
(73) Akinc, A.; Goldberg, M.; Qin, J.; Dorkin, J. R.; Gamba-Vitalo, C.; Maier, M.; Jayaprakash, K. N.; Jayaraman, M.; Rajeev, K. G.; Manoharan, M.; Koteliansky, V.; Rohl, I.; Leshchiner, E. S.; Langer, R.; Anderson, D. G. *Mol. Ther.* **2009**, *17* (5), 872−879.
(74) Lorenz, C.; Hadwiger, P.; John, M.; Vornlocher, H.-P.; Unverzagt, C. *Bioorg. Med. Chem. Lett.* **2004**, *14* (19), 4975−4977.
(75) Zuidam, N.; Posthumab, G.; de Vries, E.; Crommelin, D.; Hennink, W.; Storm, G. *J. Drug Targeting* **2000**, *8* (1), 51−66.
(76) Kwok, A.; Hart, S. L. *Nanomedicine* **2011**, *7* (2), 210−219.
(77) Won, Y.-W.; Yoon, S.-M.; Lee, K.-M.; Kim, Y.-H. *Mol. Ther.* **2011**, *19* (2), 372−380.
(78) Hermanson, G. T. *Bioconjugate Techniques*; Elsevier Inc.: Amsterdam, 2008.
(79) Yessine, M.-A.; Meier, C.; Petereit, H.-U.; Leroux, J.-C. *Eur. J. Pharm. Biopharm.* **2006**, *63* (1), 1−10.
(80) Wu, G. Y.; Wu, C. H. *J. Biol. Chem.* **1987**, *262* (10), 4429−4432.
(81) Park, T. G.; Jeong, J. H.; Kim, S. W. *Adv. Drug Delivery Rev.* **2006**, *58* (4), 467−486.
(82) Convertine, A. J.; Diab, C.; Prieve, M.; Paschal, A.; Hoffman, A. S.; Johnson, P. H.; Stayton, P. S. *Biomacromolecules* **2010**, *11* (11), 2904−2911.
(83) Kim, H.-K.; Davaa, E.; Myung, C.-S.; Park, J.-S. *Int. J. Pharm.* **2010**, *392* (1−2), 141−147.

NOTE ADDED AFTER ASAP PUBLICATION

This article posted asap on October 30, 2013. Paragraph 1, sentence 4 of the Experimental Section; Table 3; and paragraph 1, sentence 3 of the Conclusion section have been revised. The correct version posted on November 11, 2013.